Synthesis and characterization of PVDF macroinitiators with well-defined functional end-groups

N.L. Meereboer, V.S.D. Voet, G. ten Brinke, K. Loos, *MSc thesis* **2013**, Department of Polymer Chemistry, Zernike Institute for Advanced Materials, University of Groningen

university of groningen / zernike institute for advanced materials

Synthesis and characterization of PVDF macroinitiators with well-defined functional end-groups

N.L. Meereboer, V.S.D. Voet, G. ten Brinke, K. Loos, *MSc thesis* **2013**, Department of Polymer Chemistry, Zernike Institute for Advanced Materials, University of Groningen

Abstract

PVDF macroinitiators have been synthesized with functionalized initiators and characterized using ^{1}H-NMR spectroscopy. A THP-protected benzoyl peroxide was polymerized with VDF, and subsequent acidic cleavage resulted in a hydroxyl-terminated PVDF macroinitiator. From the macroinitiators, ROP was employed to obtain PLA-*b*-PVDF-*b*-PLA triblock copolymers using different catalysts.

TBD proved to be an excellent organocatalyst for LA polymerizations, since such polymerizations can be employed under mild reaction conditions and with short reaction times. Hydroxyl-terminated PS was used to optimize the experimental conditions, however when employing these reaction conditions to hydroxyl-terminated PVDF impurities initiated homopolymerization as well.

Introducing bromine functional groups to the benzoyl peroxide resulted in bromine-terminated PVDF macroinitiators after VDF polymerization. Post modification of the bromine-functionalized PVDF using sodium azide resulted in full conversion of the bromine into azide functional groups.

The azide-functionalized PVDF was subjected to a copper-catalyzed azide-alkyne cycloaddition with 1-pentyne. ^{1}H-NMR spectroscopy confirmed the click reaction by a downfield shift of the methylene signal.

Ethynyl-functionalized P3HT was synthesized using a Grignard metathesis polymerization. A molecular weight of 8000 g/mol was determined from the ratio between integrals of the ethynyl proton and aromatic proton.

First attempts of CuAAC with an azide-functionalized PVDF and an ethynyl-terminated P3HT were employed, however no successful click reaction was observed. It is believed that high purity of the P3HT block is required and that a longer linker enhances the polarization on the ethynyl bond.

Contents

1. Introduction

1.1 Multiferroics

In the past years, the understanding of multiferroic materials received an increasing amount of research attention. Besides early efforts of producing multiferroic materials,[4] wherein at least two out of three ferroic orders (ferroelectricity, ferromagnetism, and ferroelasticity) coexist in one phase, the fast development of these materials emerged upon the last decade.[5-9]

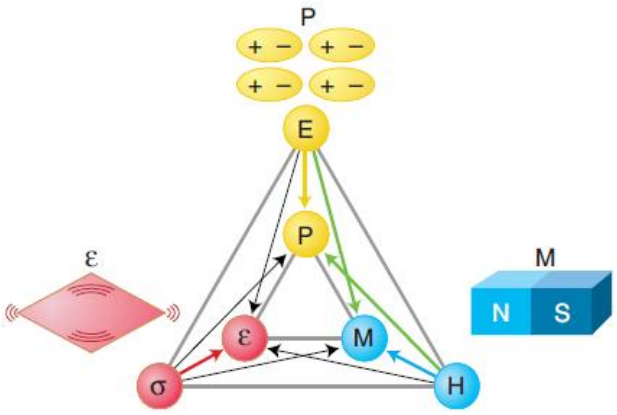

Figure 1. Ferroic and multiferroic phase control. As depicted, control of polarization *P*, magnetization *M*, and strain *ε*, by an electric field *E*, magnetic field *H*, and stress *σ*, respectively. Also, coupling between different ferroic orders are demonstrated.

In these ferroic materials, polarization, magnetization, and strain are spontaneously formed and can be reversed by applying an electric field, magnetic field, and stress, respectively. If an electric field can reverse the magnetization and a magnetic field can reverse the polarization, these materials are referred to as multiferroic magnetoelectric (Figure 1). Referring to Figure 2, the hysteresis behavior can be explained. Initially, domains of ferromagnetic order are distributed in all directions resulting in a zero magnetization. However, when applying a magnetic field, the spins of the domains are aligning in one direction, giving a final saturated magnetization ($\boldsymbol{B_s}$). Removal of the magnetic field results in a remnant magnetization ($\boldsymbol{B_r}$) characteristic for ferroic materials. By reversing the magnetic field,

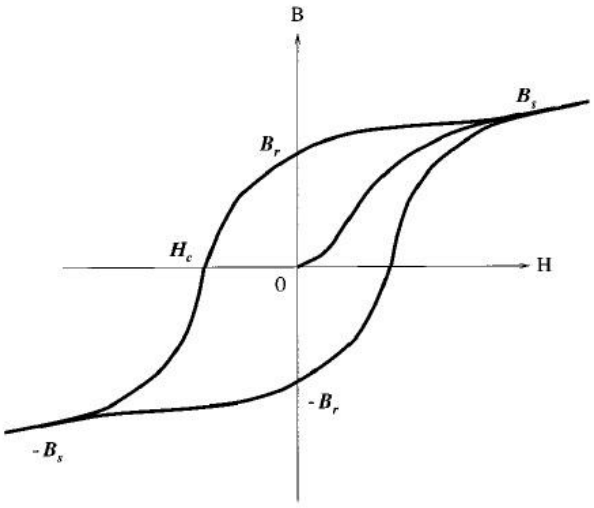

Figure 2. Hysteresis curve for a ferromagnetic material.

electron spins are turned resulting in a switched magnetization. Indeed, the magnetization remains after removing the magnetic field. Ferroelectric and ferroelastic materials demonstrate similar behavior: the polarization and strain is reversed, respectively.

This unique behavior gives rise to numerous applications. Most appealing is the use of multiferroics in data storage devices.[10] Their hysteresis behavior offers the possibility to encode data into '0' and '1' by using the two polarization states. Electrical writing and magnetic reading provides best of both materials, since fatigue (*i.e.* loss of switched charge owing to repetitive destructive read out) and retention (*i.e.* stored charge has decreased to a level where the (+) or (-) state of polarization cannot be reliably sensed) are avoided and no large local magnetic field is required to write.[9,11,12] Additional applications involve high-sensitivity magnetic field sensors and electrically tunable microwave materials.[7,13,14]

1.2 Ferroelectric polymers

For large scale production of multiferroic materials, the costs are high, the processability is limited, and the chemical resistance to solvents is not always plausible when using metal composites. In order to create low-cost processable, and solvent resistant materials, polymers are superior. Poly(vinylidene fluoride) (PVDF), known for its ferroelectric properties, is a suitable candidate to fulfill this requirements. In 1969, Kawai discovered the ferroelectric behavior of PVDF upon applying an electric field.[15]

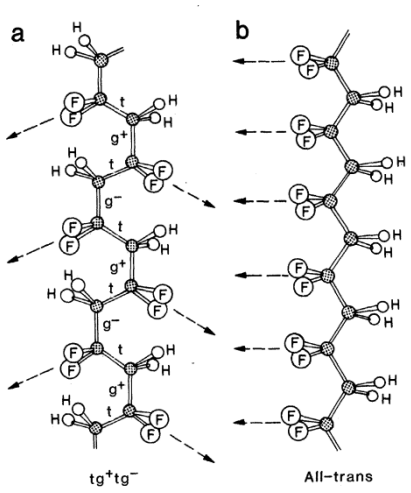

Figure 3. The two most common chain conformations of PVDF: (a) tg^+tg^- and (b) all-trans. The tg^+tg^- conformation has components of the dipole moment perpendicular and parallel to the axis, whereas the all-trans only has components normal to the axis.

The following years, intensive research on this exceptional polymer was performed. To yield a ferroelectric polymer, small monomeric units are required to obtain crystallization or to avoid crystallization into bulky shapes (*e.g.* the helical shape), because such structures will lead to cancellation of the dipole moments along the polymer chain. Furthermore, crosslinking is highly undesired, *i.e.* the ferroelectric polymer needs to be chemically

stable. The strong dipole moment between the carbon-fluorine bond and the small radius of the fluorine atom (1.35 Å) compared to the hydrogen atom (1.2 Å) makes PVDF highly appropriate to yield ferroelectric polymers. The strongest dipole moment will be achieved when head-to-tail coupling between the monomeric units is favored. Head-to-head and tail-to-tail coupling leads to a reduction of 6-10 % of the dipole moment per monomeric unit of VDF.[16]

Apart from chain configuration, also chain conformation is influencing the dipole moment. In the melt or in solution, chain conformations are randomly oriented. Nevertheless, configurationally regular parts can crystallize when cooled from the melt or when the solvent is evaporated. Due to electrostatic interactions and internal sterics, rotations around single bonds minimize the potential energy. This results in favorable torsional bond arrangements where substituents are at 180° (*t*) or at +- 60° (g^+, g^-) with respect to each other. The most abundant conformations are *all-trans*, tg^+tg^-, and $tttg^+tttg^-$. As depicted in Figure 3, the highest polar conformation is *all-trans*, since all dipoles are aligned in one direction. The tg^+tg^- chain conformation also possesses a net dipole moment along the polymer chain, however as pointed out in Figure 4, cancellation of the dipoles occur due to the antiparallel arrangement of the chains packed in the α-phase crystal lattice. The most polar and therefore most interesting unit cell is the β-phase. Herein, the strongest net dipole is observed, because dipoles of both chains in the unit cell are pointing in the same direction.

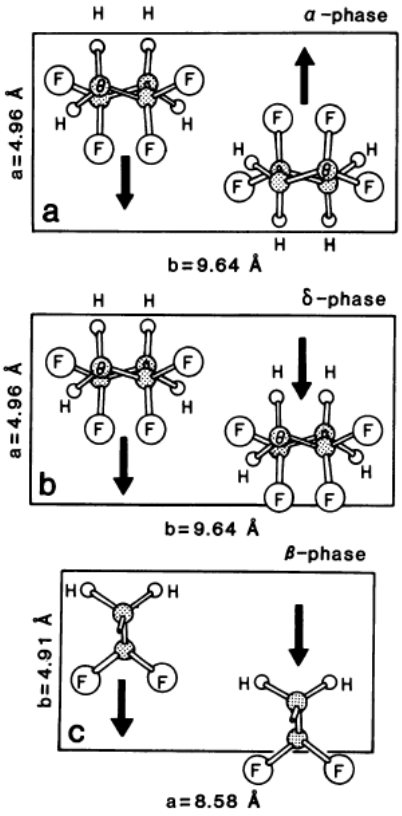

Figure 4. PVDF unit cells of the α-phase (a), δ-phase (b), and β-phase (c). The δ-phase can be obtained by applying a high electric field to PVDF in the α-phase.[2,3]

In block copolymers, the β-phase polymorph of PVDF is observed in PS-*b*-PVDF-*b*-PS [1], indicating that the *all-trans* conformation is promoted by the amorphous phase in the semicrystalline block copolymers. Moreover, polar aprotic casting solvents support the formation of the β-phase, whereas DMF demonstrated an enhanced ratio of β-phase

compared to NMP. Thus, in order to obtain a ferroelectric polymer as building block for multiferroic materials, PVDF seems to be an excellent choice due to its ferroelectric β-phase, which can be further enhanced by choosing the proper casting solvent.

1.3 Block copolymer phase behavior

Block copolymers contain two or more covalently linked polymer chains with distinct chemical composition. This special class of macromolecules tend to phase separate, however due to the fact that the blocks are covalently attached, separation only occurs at length scales ranging from 10^{-6}-10^{-9} m.[17] These materials, with precision to the nanoscale level, demonstrate their use in numerous applications such as solar cells, nanoporous membranes, and biomedical devices.[2,3,18-20]

Block copolymers microphase separate due to the unfavorable interaction between the dissimilar blocks. This enthalpic driving force is counterbalanced by a loss in translational freedom at the junction, reducing the entropy of the system.[21] This relation is expressed in the Gibbs free energy of mixing depicted in Equation 1.

$$\frac{\Delta G_{mix}}{k_B T} = \frac{f_A}{N_A} \ln f_A + \frac{f_B}{N_B} \ln f_B + f_A f_B \chi_{AB}$$

Equation 1. ΔG_{mix} is the Gibbs free energy of mixing, k_B is the Boltzmann constant, T is the temperature, f_A and f_B are the compositions of blocks A and B respectively, N_A and N_B are the number of monomers of blocks A and B respectively and χ_{AB} is the Flory-Huggins interaction parameter.

The Flory-Huggins interaction parameter (Equation 2) states the contrariness between different monomers. Hereby, a positive χ-value accounts for unfavorable interactions between monomers. In practice, the χ-value is positive for polymers if there are no strong specific interactions like hydrogen bonding or charge attraction.

$$\chi_{AB} = \frac{Z}{k_B T} [\varepsilon_{AB} - \frac{1}{2} (\varepsilon_{AA} + \varepsilon_{BB})]$$

Equation 2. χ_{AB} is the interaction parameter, Z is the number of nearest-neighbor monomers, k_B is the Boltzmann constant, T is the temperature, ε_{AB} is the interaction energy between monomer A and monomer B, same principle applies to ε_{AA} and ε_{BB}.

Hence, a positive χ and a sufficiently large N are required to obtain a microphase separated block copolymer system. A disordered state is obtained if the system is under entropic control. The critical point for a binary system is calculated at $\chi N = 10.5$, using the Self-Consistent Field Theory (SCFT). Above the Order-Disorder Transition (ODT)

point different morphologies are acquired, depending on the chain length and composition of the block copolymer.

Theoretical and experimental results have led to phase diagrams for an A-*b*-B block copolymer as is depicted in Figure 5a and Figure 5b, respectively.[22,23] Stronger segregation can be obtained by extending the chain length or increasing the interaction parameter.

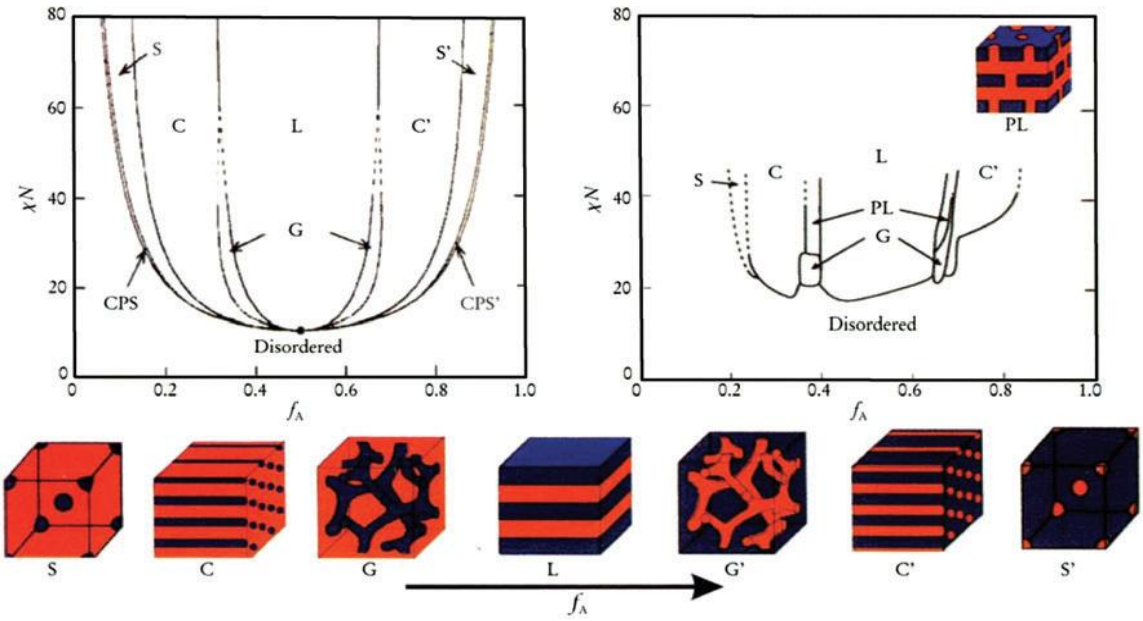

Figure 5. Theoretical (a) and experimental (b) phase diagram of an A-*b*-B block copolymer. Observed equilibrium morphologies, S (body-centered-cubic spheres), C (cylinders), G (gyroid), and L (lamellae), are depicted along the x-axis as function of the volume fraction of block A. CPS (close packed spheres) and PL (perforated lamellae) are found theoretically and experimentally, respectively.[17,24]

The experimental critical point of phase separation is found to be higher in comparison to the theoretical value.

An interesting feature of block copolymers is their ability to form different nanostructures by altering the size of the different polymer blocks. Therefore, they can be employed as precursors for functional nanomaterials. For example, by selectively removing one of the blocks, a nanoporous template is obtained, which can be backfilled with a complementary material in order to generate nanostructured composites.[1,25]

Introducing a semicrystalline block to the system creates an additional ordering process when cooling from the melt. Nanoscale structures are therefore not solely obtained due to block incompatibility, but as well by crystallization.[26] The energy of crystallization and

the energy accompanied with microphase separation differ approximately two orders of magnitude, resulting in the dominant role of crystallization during structure formation.

Often spherulites are found, and within the spherulites a lamellar structure consisting of crystalline and amorphous layers. Nevertheless, if the glass transition of an amorphous block is higher than the crystallization temperature of the semicrystalline block, confined crystallization takes place into a shape determined by the amorphous block.[27]

So far, only random coil block copolymers have been discussed. If one or both blocks behave rod-like (e.g. in the case of conjugated polymers), their self-assembly is completely different. First, the conformational entropy is dramatically reduced and the macromolecules will pack differently. Self-assembled rod-like structures are not able to accommodate packing by stretching and in solution they cannot gain conformational entropy. Furthermore, additional anisotropic interactions (*e.g.* π-π stacking) enhance the crystalline packing. In the melt or at θ-conditions, random coils have a radius of gyration (R_g) that scales as $N^{1/2}$, whereas the R_g for rod-like blocks has a linear dependency with N. This dissimilarity leads to the introduction of an additional parameter, which includes the ratio of rod and coil block lengths. Furthermore, another parameter needs to capture the orientation interaction between rods (Maier-Saupe interactions), volume fraction(s) of the rod-like block(s), and the Flory-Huggins parameter.[28-31]

1.4 PVDF-based block copolymers

Multiferroic materials based on PVDF require an additional ferromagnetic component to realize the desired product. Different strategies can be applied; among them are blending of ferroelectric homopolymer with nanoparticles to acquire polymer nanocomposites[32,33], coupling of PVDF to a ferromagnetic polymer[34] block, or preparing block copolymer composed of PVDF and a sacrificial block, to attain

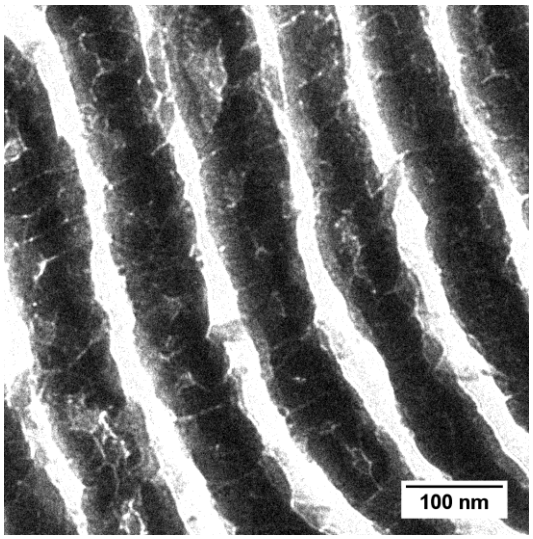

Figure 6. TEM image of a PVDF/Ni nanocomposite with a lamellar morphology, obtained after selective removal of PS from a PS-*b*-PVDF-b-PS triblock copolymer structure. The nanoporous template is backfilled with nickel.[1]

ordered structures with nanoscale precision, which can be selectively etched and subsequently backfilled with (ferromagnetic) materials of interest[1]. The removal of sacrificial blocks is demonstrated by using various etching techniques, including hydrolysis[35], UV irradiation[36,37], amphiphile extraction [25,38], and reactive ion etching[39]. In particular, the use of block copolymers seems promising, since well-defined morphologies can be obtained to produce composites with high magnetoelectric coupling constants[9].

Vanderleene *et al.* were the first to show the ferromagnetic behavior of poly(3-hexylthiophene) (P3HT). Due to large distances between spins, Curie-Weiss paramagnetic behavior was demonstrated at room temperature. Nevertheless, ferromagnetic behavior was proved by SQUID measurements at 5K.[34] Creating block copolymers of PVDF and P3HT may give rise to a new class of materials, not only because of the reported magnetic behavior of P3HT, but also due to its electronic properties.[40] For example, in FeFET (Ferroelectric Field Effect Transistors), electron trapping occurs at the ferroelectric/semiconducting interface.[41] Introducing block copolymers composed of a ferroelectric block and semiconducting block at the ferroelectric/semiconducting interface could resolve this problem.

Block copolymers based on PVDF are in general prepared *via* controlled polymerization from end-group functionalized PVDF. Different synthetic approaches have been used to prepare such PVDF macroinitiators, like ITP (Iodine Transfer Polymerization)[42,43], emulsion polymerization[44], and free radical polymerization[45]. From here, ATRP is frequently used to synthesize the adjacent block(s), depending on the amount of chain end functionalities.[42-44,46,47] Unfortunately, not all techniques described above deliver desired molecular weight, narrow polydispersities, and high end-group fidelity needed to deliver ordered nanostructures. Wang and coworkers[45] provided a new route towards telechelic fluoropolymers. Benzoyl peroxides with different functional groups were used to create a variety of end-functionalized fluoropolymers. This enables different polymerization techniques for creating block copolymers, like ATRP and ROP. Moreover, due to high end-group fidelity, post modification can be applied to convert the end-groups into different functionalities.

1.5 Click chemistry

The development of well-defined nanostructures has gained an enormous boost in recent years due to 'click' chemistry. The groups of Sharpless[48] and Meldal[49] independently developed a versatile tool to click (covalently link) different molecules *via* so-called Cu-catalyzed Azide Alkyne Cycloaddition (CuAAC). Simplicity and robustness are key words for this method, allowing various research fields to apply CuAAC for manufacturing well-architectured molecules, such as block copolymers.[50]

Extensive research into the reaction mechanism of CuAAC revealed that a product in high purity and high yield is obtained by affording a variety of reaction conditions.[51] Additionally, tolerance to numerous functional groups enables one-step synthesis without any protecting and deprotecting steps.[52]

PVDF-containing block copolymer synthesis based on CuAAC has hardly been studied in the literature. Nevertheless, Vukicevic *et al.*[53] reported CuAAC of azide-functionalized (low molecular weight) PVDF and alkyne-terminated polystyrene (PS).

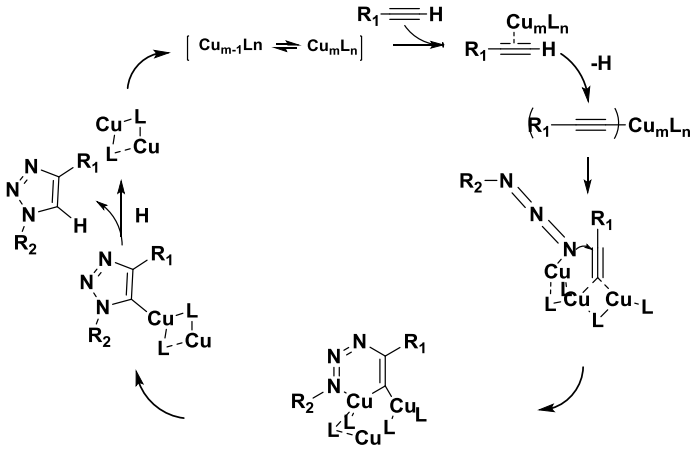

Figure 7. A plausible catalytic pathway for CuAAC proposed by Meldal *et al.* [52]

On the other hand, alkyne-terminated P3HT can be obtained *via* a convenient synthesis route, using Grignard metathesis polymerization (GRIM).[54] Urien *et al.*[55] were the first to demonstrate CuAAC for P3HT and PS. Furthermore, Li *et al.*[56] reported the formation of P3HT-*b*-PAA. Striking is the straightforward conversion of the bromine end-group of the precursor (PtBA-Br) into an azide functional group. Whereas synthetic

procedures proposed by Li and Urien lead to relatively low molecular weight P3HT (< 8200 g/mol), Lohwasser and Thelakkat[57] reported that the P3HT block in P3HT-*b*-P4VP can be prepared with a molecular weight of 19200 g/mol by a modified GRIM method. Increasing the chain length of P3HT enhances the crystallization process, which in turn leads to better charge transport. Due to the high regioregularity of the alkyl side chains in the P3HT backbone, besides the intramolecular charge transport, also intermolecular π-π stacking contributes to the charge transport.[58,59]

Hence, block copolymer click chemistry has been employed for both PVDF and P3HT. Combining both blocks *via* CuAAC is a promising route to obtain novel block copolymers with unique properties.

1.6 Ring opening polymerization of poly(lactid acid)

Belonging to the class of aliphatic polyesters, poly(lactic acid) (PLA) is a semicrystalline polymer with a glass transition of 55°C and melting temperature of 175°C. Its monomer, lactide (LA), has three optical active isomers: D-lactide, L-lactide, and D,L,-lactide. The degree of crystallinity of the polymer can be tuned by varying the fraction of these isomers.[60]

Polymerization *via* ring opening (ROP) is the common tool to acquire these (bio)degradable, biocompatible polymers.[61,62] Ring opening is in general initiated by either an alcohol or amine functional group, and the desired molecular weight can be altered by varying the monomer to initiator ratio. Stannous(II)octoate (tin(II) 2-ethylhexanoate) is the most widely used catalyst, due to its high conversion rate, high reaction rate, and high molecular weight products.[63] Nevertheless, a detailed study of stannous(II)octoate demonstrated the contamination with 2-ethyl hexanoic acid, and removing this contaminant by distillation proved to be challenging. Moreover, aging in the flask leads to even more impurities.[64] Block copolymer formation through ROP cannot afford other reactive species in the mixture besides the macroinitiator, monomer, and catalyst. Because of the complexity of metallic initiators, the presence of impurities and the high temperatures required to polymerize lactide, an escape route towards more predictable catalysts is desirable.

Lohmeijer *et. al.*[65] reported the polymerization of various cyclic esters by using different organic catalysts at room temperature. 1,5,7-triazabicyclo[4.4.0]dec-5-ene, 7-methyl-1,5,7-triazabicyclo[4.4.0]dec-5-ene, 1,8-diazabicyclo[5.4.0]undec-7-ene (TBD, MTBD, DBU, respectively) were used to synthesize PLA within a few hours or even a few seconds. Molecular weights up to 85000 g/mol were achieved with molecular weight distributions close to 1.0. TBD was found to be the most active catalyst, since dual activation of both monomer and initiator/propagating chain occur in close proximity (Figure 8).

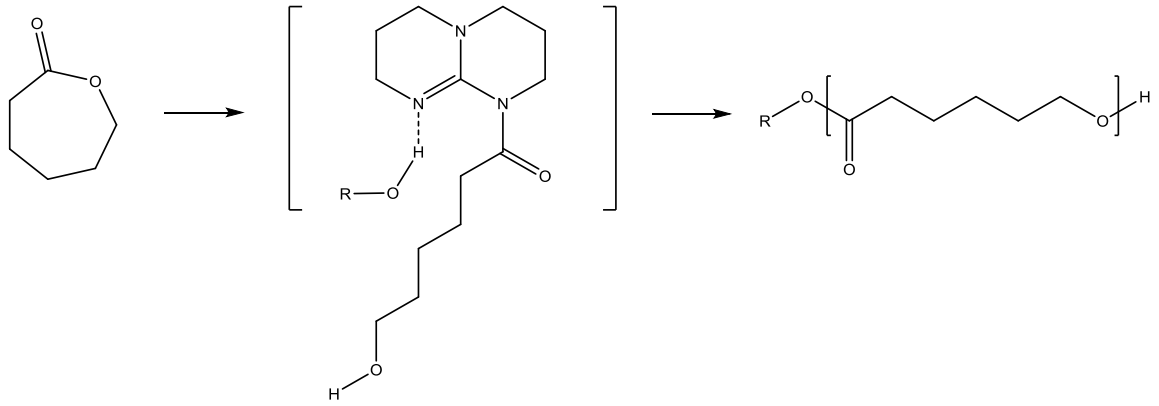

Figure 8. Ring-Opening Polymerization of Caprolactone through Dual Activation by TBD.[65]

Block copolymers containing PLA as secondary block were formed *via* ring opening of hydroxyl-terminated PS, where TBD was used as catalyst.[65] The group of Hedrick demonstrated sequential polymerization by first applying a nitroxide mediated polymerization (NMP) and subsequently ROP using thiourea and tertiary amine catalysts.[66,67] Furthermore, PS-*b*-PLA shear aligned hexagonally packed cylindrical nanostructures were selectively etched using a 0.5M NaOH in MeOH/H_2O (40/60) solution, resulting in a nanoporous hydrophilic PS matrix. Noteworthy, the catalyst used for this sequential polymerization is $AlEt_3$.[68]

1.7 Project description

1.7.1 Ring Opening Polymerization

For ongoing research into the intriguing properties and the potential applications of PVDF, it is desirable to gain access to numerous polymerization techniques. The most common technique used to generate block copolymers based on PVDF is employing ATRP from a PVDF backbone. Altering the initiator for PVDF polymerizations results in different end functionalized PVDF macroinitiators,[45] which enables the use of different polymerization techniques, like ROP.

To pave this way, the first goal of this project is synthesizing hydroxyl-terminated PVDF macroinitiators, from which ROP can be employed. In order to achieve this goal, THP-protected benzoyl peroxides will be synthesized following the procedure of Li *et. al*.[45] In this manner well-defined PVDF macroinitiators are prepared, which has also been demonstrated using chlorine functionalized PVDF by Voet *et. al.*[1]. Deprotecting PVDF by hydrolysis using a strong acidic solution should result in hydroxyl-terminated PVDF chains.

When the hydroxyl-capped PVDF macroinitiators are obtained, ROP will be employed. Due to limited availability, the high sensitivity to moisture and the restriction of using DMF as solvent, first homopolymerizations will be employed by mimicking the end group of PVDF and using stannous octoate as catalyst to gain knowledge about the reaction conditions. In addition, various organic catalysts will be investigated, following the promising work of Lohmeijer *et.al.*.[65]

1.7.2 P3HT-*b*-PVDF-*b*-P3HT

Thiophene end-capping of hydroxyl-terminated PVDF macroinitiators will be the first approach to synthesize P3HT-*b*-PVDF-*b*-P3HT block copolymers. Esterification of the hydroxyl groups with thiophene-2-carboxyl chloride provides the possibility for oxidative polymerization with 3-hexyl thiophenes from the resulting PVDF macroinitiator.[69]

A different synthetic approach towards P3HT-*b*-PVDF-*b*-P3HT block copolymers will include azide-alkyne coupling, or so-called click chemistry. By independently synthesizing the P3HT and PVDF macroinitiators, control over molecular weight and polydispersity enables a promising route towards well-defined block copolymers. The alkyne functionality in P3HT required for CuAAC is already introduced by the McCullough group.[54] A route towards azide-functionalized PVDF includes the conversion of the bromine-terminated PVDF into an azide functionality, usually achieved by reacting with sodium azide. In order to acquire PVDF with an end-capped bromine, a new initiator will be developed with bromine functionality.

2. Experimental

2.1 Materials

1,8-Diazabicyclo[5.4.0]undec-7-ene (DBU, 98%, Acros Organics), 1,5,7-triazabicyclo[4.4.0]dec-5-ene (TBD, 98%, Sigma-Aldrich), 7-methyl-1,5,7-triazabicyclo[4.4.0]dec-5-ene (MTBD, 98%, Sigma-Aldrich), N,N'-dicyclohexylcarbodiimide (1M solution in DCM, Acros Organics), vinylidene fluoride (VDF, 98%, Synquest Labs), pyridinium p-toluenesulfonate (98%, Acros Organics), methyl 4-(hydroxymethyl)benzoate (Sigma-Aldrich), 3,4-dihydro-2H-pyran (97%, Sigma-Aldrich), tin-2-ethylhexanoate (stannous(II)octoate, 95%, Sigma-Aldrich), dimethylformamide (DMF, >99%, Acros Organics), dichloromethane (DCM, >99.8%, anhydrous, Sigma-Aldrich), hydrogen peroxide (ACS reagent, 30 wt. % solution in H_2O, non-stabilized, Acros Organics), potassium hydroxide (85%, Acros Organics), acetic acid (99.5%, Acros Organics), hydrogen chloride (37% sol., Merck), 4-(bromomethyl)benzoic acid (97%, Acros Organics), oxalyl chloride (98%, Acros Organics), anhydrous DCM (99.8%, Acros Organics), anhydrous DMF (99.8%, Sigma-Aldrich), lithium peroxide (95%, Acros Organics), chloroform (99.5%, stb. Ethanol, Poch S.A.), 1-pentyne (99%, Sigma-Aldrich), *n*-hexanes (99%, Poch S.A.), polystyrene-OH (M_w=2900, M_n=2200, Polymer Scource Inc.), sodium azide (99.5%, Sigma-Aldrich), copper(I)bromide (98%, Sigma-Aldrich), 1,1,4,7,7-pentamethyldiethylenetriamine (PMDETA, 99%, Acros Organics), [1,3-bis(diphenylphosphino)propane]dichloronickel(II) (Sigma-Aldrich), 2,5-dibromo-3-hexylthiophene (97%, Sigma-Aldrich), 3-hexyl thiophene (99%, Sigma-Aldrich), thiophene 3-carboxyl chloride (97%, Sigma-Aldrich), i-propylmagnesiumchloride (2.0 M in THF, Sigma-Aldrich), ethynyl magnesium bromide (0.5 M in THF) were all used as received. 3,6-dimethyl-1,4-dioxane-2,5-dione (LA, D,L-lactide, 99%, Acros Organics) was recrystallized from ethylacetate. All solvents used were of analytical grade.

2.2 Characterization

^{1}H nuclear magnetic resonance (^{1}H-NMR) spectra were recorded on a 400 MHz Varian VXR operating at room temperature. Gel permeation chromatography (GPC) was performed in DMF (1 mL min^{-1}) with 0.01 M LiBr on a Viscotek GPCMAX equipped with model 302 TDA detectors, using two columns (PSS-Gram-1000/30, 10 μ 30 cm). Molecular weights were calculated relative to polystyrene according to universal calibration using narrow disperse standards (Polymer Laboratories).

2.3 Experiments

2.3.1 Hydroxyl-terminated PVDF

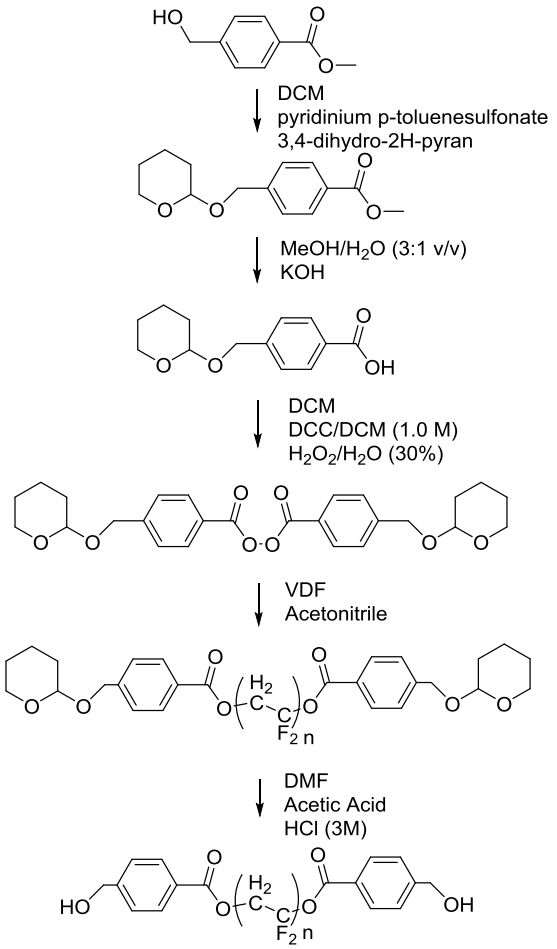

Scheme 1. Synthetic pathway towards hydroxyl-functionalized PVDF.

Synthesis of [(tetrahydropyran-2-yloxy)methyl]benzoate

In a 500 mL three-necked round-bottom flask 0.627 g (2.50 mmol) pyridinium *p*-toluenesulfonate and 3.25 mL (35.6 mmol) 3,4-dihydro-2H-pyran were added under a N_2 atmosphere to a stirred solution of 4.00 g (24.1 mmol) methyl 4-(hydroxymethyl) benzoate in 180 mL anhydrous DCM. This clear solution was stirred for 19 hours at room temperature. Thereafter, dilution with 120 mL diethylether followed and the mixture was washed twice with 50 mL brine. Extraction of the aqueous phase twice with 50 mL diethylether followed and both organic phases were combined and dried over $MgSO_4$. After filtration, concentration *in vacuo* yielded 5.1 g (20.4 mmol, 84.6%) white product.^{1}H-NMR (400 MHz, $CDCl_3$, δ): 8.02 (d, 2H, ArH), 7.42 (d, 2H, ArH), 4.83 (d, 1H), 4.69 (t, 1H), 4. 55 (d, 1H), 3.93-3.85 (m, 1H), 3.90 (s, 3H), 3.57-3.50 (m, 1H), 1.91-1.52 (m, 6H).

Synthesis of [(tetrahydropyran-2-yloxy)methyl]benzoic acid

A slightly yellow solution was obtained after addition of 4.805 g (19.2 mmol) [(tetrahydropyran-2-yloxy)methyl]benzoate, 2.16 g KOH, and 155 mL 3:1 v/v MeOH/H_2O to a 250 mL round-bottom flask. After stirring for 18 hours at room temperature, methanol was evaporated (50°C, 200 mbar). A 3M HCl solution was prepared and added dropwise in order to let the product precipitate. Dropwise addition was maintained until a drop in pH was observed. Filtration and drying *in vacuo* at 40°C yielded 3.26 g (13.8 mmol, 72%) of white product.^{1}H-NMR (400 MHz, d_6-DMSO, δ): 7.91 (d, 2H, ArH), 7.44 (d, 2H, ArH), 4.73 (d, 1H), 4.70-4.65 (m, 1H), 4.51 (d, 1H), 3.82-3.72 (m, 1H), 3.51-3.42 (m, 1H), 1.80-1.40 (m, 6H).

Synthesis of [(tetrahydropyran-2-yloxy)methyl]benzoyl peroxide

To a stirred solution of 0.956 g (4.05 mmol) [(tetrahydropyran-2-yloxy)methyl]benzoic acid and 16 mL DCM was added a mixture of 4.2 mL 1.0 M DCC solution in DCM and

2.6 mL (30%) H_2O_2/H_2O at 0°C. The resulting white dispersion was stirred for 5 hours at room temperature. Subsequently, the mixture was diluted with 40 mL DCM and the white precipitate was removed by filtration. The organic phase was washed with 60 mL H_2O and 60 mL brine. Subsequently drying over $MgSO_4$, filtration, concentration *in vacuo* (620 mbar, 35°C), and drying *in vacuo* at room temperature yielded a white product (0.461 g, 0.981 mmol, 48%).^{1}H-NMR (400 MHz, $CDCl_3$, δ): 8.06 (d, 2H, ArH), 7.51 (d, 2H, ArH), 4.87 (d, 1H), 4.73 (t, 1H), 4.60 (d, 1H), 3.95-3.85 (m, 1H), 3.60-3.52 (m, 1H), 2.00-1.50 (m, 6H).

Synthesis of PVDF end-capped with tetrahydropyran protecting group

To a pressure reactor (Parr Instruments, model 4568) was added 0.207 g (0.440 mmol) [(tetrahydropyran-2-yloxy)methyl]benzoyl peroxide and 110 mL anhydrous ACN. The vessel was closed and the solution was purged with N_2 to degas the mixture for 30 minutes. Thereafter, the reactor was charged with 20 bar VDF, heated to 90°C and stirred at 500 rpm. After 2 hours, the vessel was cooled down to room temperature and depressurized. Cooling to 6°C resulted in a precipitate, which was collected by filtration. Washing with ACN and drying *in vacuo* at 40°C yielded 1,10 g (0.048 mmol) white product.^{1}H-NMR (400 MHz, d_6-DMSO , δ): 7.98 (d, -Ar*H*), 7.51 (d, -Ar*H*), 4.78-4.51(m, -COOC*H*$_2$CF$_2$-, -OC*H*$_2$Ar, -OC*H*O-), 3.76 (m, -CH$_2$C*H*$_2$O-), 2.87 (t, -CF$_2$C*H*$_2$-CF$_2$CH$_2$-, head-to-tail), 2.23 (t, -CF$_2$C*H*$_2$-CH$_2$CF$_2$-, tail-to-tail), 1.82-1.40 (m, -C*H*$_2$C*H*$_2$C*H*$_2$-).

Synthesis of hydroxyl-terminated PVDF

To a 500 mL round-bottom flask 0.605 g (0.027 mmol) THP-protected PVDF was dissolved in 200 mL DMF. In addition, 80 mL acetic acid and 20 mL 3M HCl were added. The solution was stirred at 60°C for 3 hours and subsequently concentrated by rotary evaporation. Precipitation in H_2O followed and the white precipitate was filtrated and washed with H_2O. Drying *in vacuo* at 40°C yielded 0.475 g (0.0208 mmol) white product. ^{1}H-NMR (400 MHz, d_6-DMSO , δ): 7.96 (d, -Ar*H*), 7.48 (d, -Ar*H*), 4.64 (m, -

COOCH_2CF$_2$-), 4.59 (s, -OCH_2Ar-), 2.87 (t, -CF$_2$CH_2-CF$_2$CH$_2$-, head-to-tail), 2.23 (t, -CF$_2$CH_2-CH$_2$CF$_2$-, tail-to-tail).

2.3.2 Ring opening polymerizations

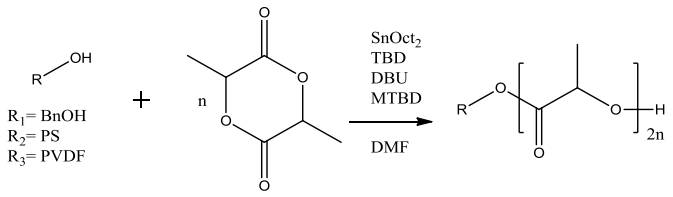

Scheme 2. Ring opening polymerization of lactide using three different initiators: benzyl alcohol, hydroxyl-terminated PS and bifunctional hydroxyl-terminated PVDF.

Synthesis of PLA using stannous octoate as catalyst

A three-necked round-bottom flask charged with a magnetic stirrer was oven-dried prior to use. The flask was charged with 0.0054-0.0186 g (0.05-0.172 mmol) benzyl alcohol, 8.75 mL dry DMF or dry toluene, 0.036-0.11 g (0.09-0.26 mmol) stannous(II)octoate and 1.25-1.47 g (8.73-10.2 mmol) LA under a N_2 outflow. The reaction mixture was submerged in a preheated oil bath at 80°C or 110°C and the reaction was stirred for 3, 24, or 72 hours. The reaction conditions are summarized in Table 1. The mixture was concentrated *in vacuo* prior to precipitation in heptane. A white solid was obtained after filtration, washing with H_2O, and drying *in vacuo*. ^{1}H-NMR (400 MHz, $CDCl_3$, δ) 5.10 (m, C*H*CH$_3$), 1.49 (m, CHC*H$_3$*).

Table 1. Overview of the experimental conditions for the optimization of the ROP using stannous(II)octoate as catalyst.

Initiator	Initiator (mmol)	Lactide (mmol)	Cat (mmol)	Solvent	Reaction volume (mL)	Temperature (°C)	Reaction time (h)	Conversion[a]
BnOH	0,050	9,30	0,15	DMF	8,75	80	3	18.6
BnOH	0,020	8,73	0,09	Toluene	8,75	110	3	100
BnOH	0,172	9,30	0,26	DMF	8,75	80	3	16.3
BnOH	0,172	9,30	0,26	DMF	8,75	110	3	33.4
BnOH	0,172	9,18	0,26	DMF	8,75	110	24	66.8
BnOH	0,172	8,81	0,15	Cyclohexanone	8,75	110	24	0
BnOH	0,172	10,2	0,26	DMF/Cyclohexanone	8,75	110	72	0

a: ^{1}H-NMR spectroscopy was used to calculate the conversion by comparing the relative intensities of the α-hydrogen signal of lactide and the polymer backbone.

Synthesis of PS-b-PLA using organocatalysts

A 50 mL three-necked round-bottom flask charged with magnetic stirrer was oven-dried prior to use. After evacuating and backfilling with N_2 for three times the flask was charged with 0.108 g (0.040 mmol) OH-terminated PS and 0.33 g (2.3 mmol) LA. Three repetitive cycles of evacuating and backfilling with N_2 were performed. After charging the flask with 4 mL DMF, five freeze-pump-thaw cycles were employed. A clear solution was obtained and 0.3 mg (0.02 mmol) TBD was added at room temperature. After 12 minutes, the mixture was quenched with 5 mg (0.04 mmol) benzoic acid. Subsequently, precipitation in H_2O and collection by filtration resulted in a solid white product. Nevertheless, a milky substance went through the filter. The same procedure was followed using MTBD (5.0 μL, 0.035 mmol) and DBU (5 μL, 0.034 mmol) as organocatalyst. ^{1}H-NMR (400 MHz, $CDCl_3$, δ, TBD as catalyst): 7.10 (m, -Ar*H*), 6.60 (m, Ar*H*), 5.16 (m, -C*H*CH_3), 1.87 (m, -CH_2CH), 1.62-1.22 (m, CHCH_3 and -CH_2C*H*).

Synthesis of PLA-b-PVDF-b-PLA using stannous(II)octoate as catalyst

A Schlenk flask was subsequently charged with 3.25 mL dry DMF, 0.163 g (0.007 mmol) hydroxyl-terminated PVDF, 0.8 g (5.5 mmol) LA, and 0.66 mL (0.1 M in DMF) stannous(II)octoate. After three freeze-pump-thaw cycles the reaction mixture was heated to 110°C and a yellowish clear solution was observed. After 168 hours the reaction was quenched by removing the oil bath and reaction mixture was precipitated in MeOH/H_2O (1:1). The crude product was obtained by filtration and subsequently washed with H_2O. An off-white powder was obtained after drying *in vacuo*. ^{1}H-NMR (400 MHz, d_6-DMSO, δ): 5.18 (m, C*H*CH_3), 2.87 (t, -CF_2C*H*$_2$-CF_2CH_2-, head-to-tail), 2.22 (t, -CF_2C*H*$_2$-CH_2CF_2-, tail-to-tail), 1.45 (m, CHC*H*$_3$).

Synthesis of PLA-b-PVDF-b-PLA using TBD

A three-necked round-bottom flask equipped with septum was thoroughly dried by repeatedly evacuating and backfilling with N_2. The flask was subsequently charged with 0.1 g (0.005 mmol) hydroxyl-terminated PVDF and 0.1 g (0.69 mmol) LA and four cycles of evacuating and backfilling with N_2 were employed. After addition of 4 mL dry DMF, three freeze-pump-thaw cycles were employed. The reaction mixture immediately turned blue and after a few minutes became brown after addition of a spatula tip TBD. After 1 hour the reaction was quenched with benzoic acid. The reaction mixture was concentrated *in vacuo* prior to precipitation in H_2O. The crude product was collected by filtration and subsequently washed with MeOH. After drying *in vacuo* 0.087 g off-white product was obtained. ^{1}H-NMR (400 MHz, d_6-DMSO , δ): 5.18 (m, C*H*CH_3), 2.87 (t, -CF_2C*H*$_2$-CF_2CH_2-, head-to-tail), 2.22 (t, -CF_2C*H*$_2$-CH_2CF_2-, tail-to-tail), 1.45 (m, CHC*H*$_3$).

2.3.3 Click chemistry

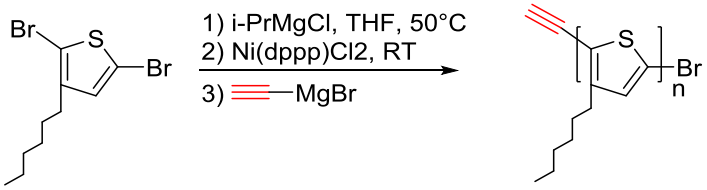

Scheme 3. Synthetic route towards ethynyl-functionalized P3HT.

Synthesis of alkyne-terminated P3HT

A 50 mL three-necked round-bottom flask charged with a magnetic stirrer was oven-dried prior to use. Three repetitive cycles of evacuating and backfilling with N_2 were employed. Under a N_2 atmosphere 0.32 mL (1.51 mmol) 2,5-dibromo-3-hexylthiophene and 12 mL dry THF was added. Dropwise addition of 0.75 mL (2.0 M in THF) i-propylmagnesiumchloride resulted in a slightly yellow solution. The mixture was stirred for 2 hours at 50°C and an orange solution was obtained. After cooling down to room temperature, 16.6 mg (2.0 mol %) Ni(dppp)Cl_2 was added resulting in a dark purple solution. The polymerization was terminated after 10 minutes by addition of 0.4 mL (0.5 M in THF) ethynyl magnesium bromide. In order to precipitate the product, 30 mL MeOH was poured into the mixture. The purple precipitate was filtrated and subsequently washed twice with MeOH, twice with *n*-hexanes and once with MeOH. Extraction of the solid phase with $CHCl_3$ and concentration *in vacuo* (500 mbar, 30°C) yielded 60.8 mg purple product. ^{1}H-NMR (400 MHz, $CDCl_3$, δ): 6.98 (s, 1H, HT-HT), 6.90 (m, 1H), 3.53 (s, 1H, ethynyl), 2.81 (t, 2H), 1.71 (t, 2H), 1.40 (m, 6H), 0.92 (t, 3H).

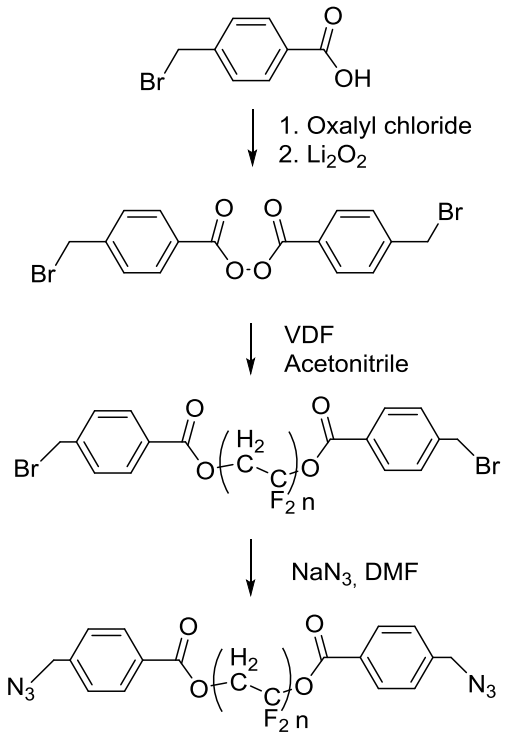

Scheme 4. Synthetic pathway towards azide-functionalized PVDF.

Synthesis of 4-(bromomethyl)benzoyl peroxide

To a stirred yellow suspension of anhydrous DCM and 2.52 g (11.7 mmol) 4-(bromomethyl)benzoic acid, 1.08 mL (12.6 mmol) oxalyl chloride and a few drops of anhydrous DMF were added at 0 °C. Stirring for 2 hours at room temperature resulted in slightly turbid solution. Immediately after concentration *in vacuo,* the remaining yellow residue was dissolved in 100 mL *n*-hexane/EtOH (1:1). Dropwise addition of the resulting solution *via* a droplet funnel to a vigorously stirred solution of 0.69 g (15.7 mmol) Li_2O_2 in 10 mL H_2O at 0 °C, resulted, after 2 hours reacting at room temperature, in a two phase mixture with a white foam on top. After dilution with 50 mL chloroform, washing twice with 40 mL H_2O followed. The aqueous phase was extracted twice with 50 mL chloroform. The combined organic phases were dried over $MgSO_4$ and removal of chloroform resulted in a white solid. Recrystallization in chloroform yielded white needles (0.495 g, 1.16 mmol).^{1}H-NMR (400 MHz, d_6-DMSO, δ): 8.02 (d, 4H, Ar*H*), 7.70 (d, 4H, Ar*H*), 4.80 (s, 4H, -C*H*$_2$Br).

Synthesis of bromine-terminated PVDF

To a pressure reactor (Parr Instruments, model 4568) 0.495 g (1.16 mmol) 4-(bromomethyl)benzoyl peroxide and 300 mL anhydrous ACN was added. The vessel was closed and the solution was purged with N_2 to degas the mixture for 30 minutes. Thereafter, the reactor was charged with 20 bar VDF, heated to 90°C and stirred at 500 rpm. After 1 hour the vessel was cooled down to room temperature and depressurized. The crude product was collected by filtration and washed twice with ACN and twice with MeOH. The solid was dissolved in DMF and precipitated in MeOH/H_2O (3:5). Collection by filtration was followed by thoroughly washing once with MeOH and five times with $CHCl_3$. The product was dried *in vacuo* at 40°C and yielded 5.6 g (0.243 mmol). ^{1}H-NMR (400 MHz, d_6-DMSO , δ): 8.00 (d, -Ar*H*), 7.63 (d, -Ar*H*), 4.76 (s, -C*H*$_2$Br), 4.64 (m, -COOC*H*$_2$CF$_2$-), 2.87 (t, -CF$_2$C*H*$_2$-CF$_2$CH$_2$-, head-to-tail), 2.23 (t, -CF$_2$C*H*$_2$-CH$_2$CF$_2$-, tail-to-tail).

Synthesis of azide-terminated PVDF

A 50 mL round-bottom flask was charged with 200 mg (0.00870 mmol) bromine-terminated PVDF, 3.4 mL DMF, and 30 mg (0.46 mmol) NaN_3. The slightly yellow solution was stirred for 18 hours at 50°C. The product was precipitated in H_2O, collected by filtration, and washed twice with MeOH. The product was dried *in vacuo* at 40°C. ^{1}H-NMR (400 MHz, d_6-DMSO , δ): 8.02 (d, -Ar*H*), 7.53 (d, -Ar*H*), 4.64 (m, , -COOC*H*$_2$CF$_2$-), 4.58 (s, -C*H*$_2$N$_3$), 2.87 (t, -CF$_2$C*H*$_2$-CF$_2$CH$_2$-, head-to-tail), 2.23 (t, -CF$_2$C*H*$_2$-CH$_2$CF$_2$-, tail-to-tail).

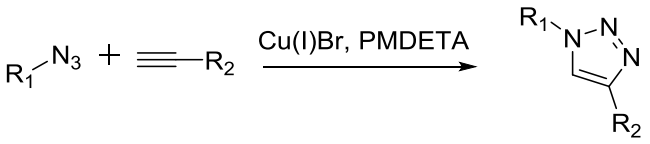

R_1 = PVDF
R_2= 1-pentyne, P3HT

Scheme 5. Synthetic route towards a PVDF-based triblock copolymer *via* CuAAC.

Synthesis of P3HT-b-PVDF-b-P3HT via a click reaction

A 50 mL three-necked round-bottom flask charged with a magnetic stirrer was oven-dried prior to use. The flask was attached to a vacuum-nitrogen line and equipped with a septum. Three repetitive cycles of evacuating and backfilling with N_2 were performed to minimize the O_2 content. The flask was charged with 120 mg (0.006 mmol) azide-terminated PVDF, 63 mg (0.012 mmol) alkyne-terminated P3HT, and 1.5 mg (0.010 mmol) Cu(I)Br. Three repetitive cycles of evacuating and backfilling with N_2 were performed. Subsequently, the flask was charged with 9.3 mL dry DMF, 9.3 mL dry $CHCl_3$, and 2.4 μL (0.011 mmol) PMDETA. A dark green suspension appeared. Three freeze-pump-thaw cycles were employed, and subsequently the mixture was heated to 40°C, and stirred for 48 hours. Removal of $CHCl_3$ and DMF by rotary evaporation resulted in a dark purple solid. After pouring MeOH into the flask and stirring for 18 hours a blue suspension appeared. The solid was collected by filtration and the crude product was mixed with *n*-hexanes. After stirring for 4 hours, the mixture was filtrated and the residue was dissolved in 50 mL $CHCl_3$. The remaining solid was removed by filtration and the filtrate was concentrated *in vacuo* yielding 5 mg of product.

2.3.4 Oxidative polymerization

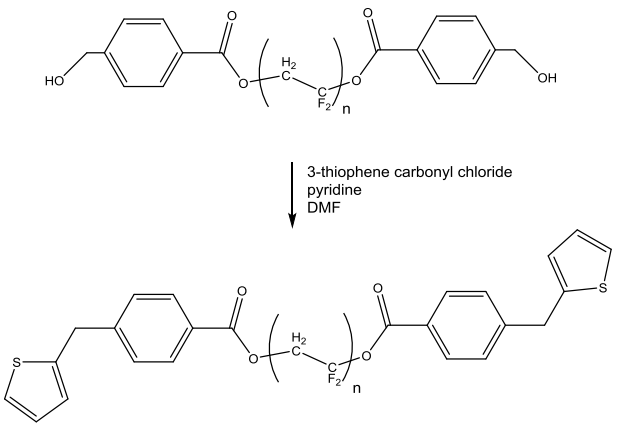

Scheme 6. Synthetic pathway towards thiophene-terminated PVDF.

Synthesis of thiophene-terminated PVDF

A 25 mL round-bottom flask was charged with 0.5 g (0.0220 mmol) hydroxyl-terminated PVDF, 15 mL DMF, 0.2 mL pyridine. Subsequently, 78 mg (0.93 mmol) 3-thiophene carbonyl chloride was added dropwise at 0°C and the salt precipitated immediately. The yellow reaction mixture was stirred at room temperature for 2 hours. After filtration, the reaction mixture was precipitated in H_2O, collected by filtration, and washed twice with dilute HCl and once with $NaHCO_3$. The product was dried *in vacuo* at 40°C and yielded 0.11 g (0.048 mmol) ^{1}H-NMR (400 MHz, d_6-DMSO , δ): 8.00 (d, -Ar*H*), 7.63 (d, -Ar*H*), 7.23 (m, -Ar*H*), 4.84 (s, -COOC*H*$_2$Ar), 4.64 (m, -COOC*H*$_2$CF$_2$-), 2.87 (t, -CF$_2$C*H*$_2$-CF$_2$CH$_2$-, head-to-tail), 2.23 (t, -CF$_2$C*H*$_2$-CH$_2$CF$_2$-, tail-to-tail).

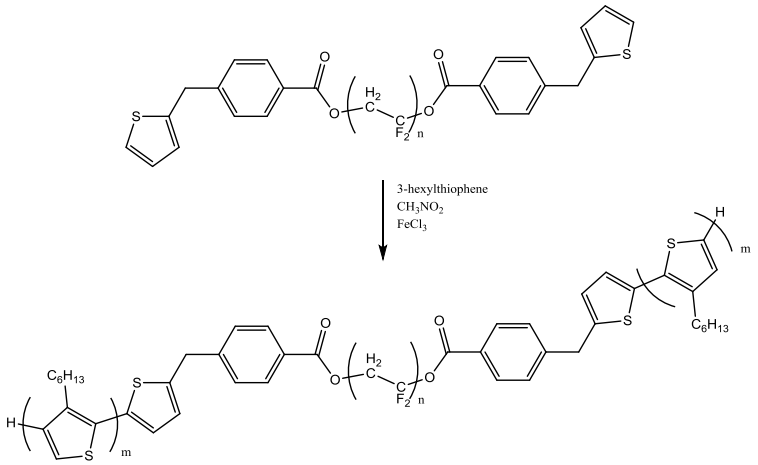

Scheme 7. Synthetic pathway towards P3HT-*b*-PVDF-*b*-P3HT *via* oxidative polymerization.

Synthesis of P3HT-b-PVDF-b-P3HT

A three-necked round-bottom flask was charged with 0.11 g thiophene-terminated PVDF, 13.5 mL nitromethane, and 0.81 g $FeCl_3$ under a N_2 atmosphere. The brown suspension was stirred for 3 hours. Subsequently, 10 mL (5% v/v) 3HT/nitromethane was added dropwise and the reaction mixture turned black immediately. After 24 hours, 20 mL of methanol was added and the reaction mixture was stirred for an additional 2 hours. After filtration, the crude product was washed with MeOH four times. The crude product was dissolved in DMSO and precipitated in MeOH. The black product was dried and analyzed with ^{1}H-NMR spectroscopy. Unfortunately, no polymer was observed in the ^{1}H-NMR spectrum.

3. Results and discussion

3.1 Hydroxyl-terminated PVDF

The synthesized [(tetrahydropyran-2-yloxy)methyl]benzoate was characterized using ^{1}H-NMR. Referring to Figure 8, the ^{1}H-NMR of the starting material demonstrated characteristic signals for the aromatic protons (7.43 ppm (d, 2H); 8.02 ppm (d, 2H)), the methylene (4.76 ppm (s, 2H)), and the methyl ester (3.91 ppm (s, 3H)). Introducing a THP protecting group results in the splitting of the methylene signal into two doublets (4.83 and 4.55 ppm), whereas the proton next to the oxygen in the THP ring shows a triplet (4.69 ppm) in the ^{1}H-NMR spectrum. Furthermore, the multiplet in between 1.91 and 1.52 ppm is characteristic for the other protons of the THP ring.

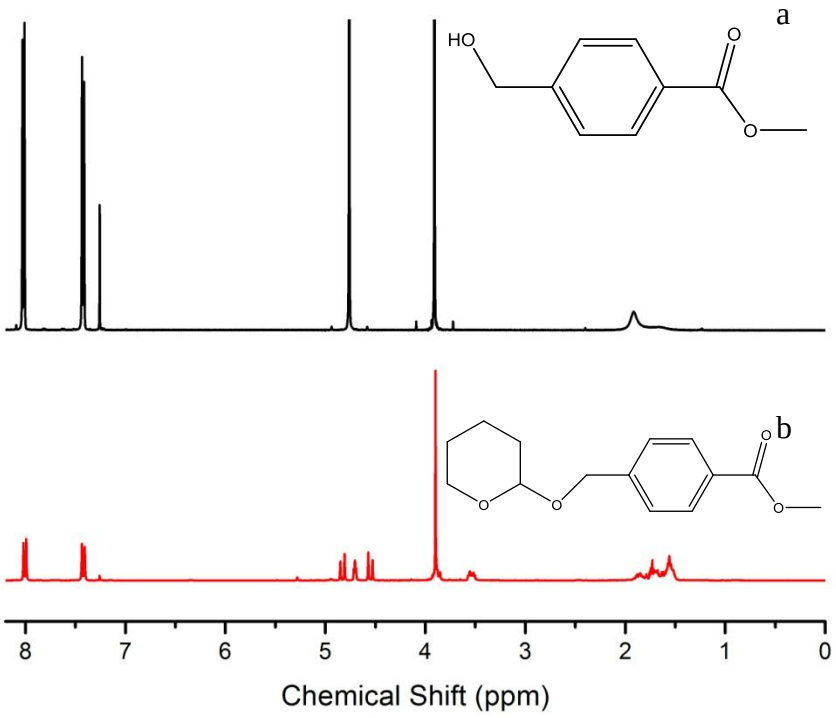

Figure 8. ^{1}H-NMR spectra of (a) methyl 4-(hydroxymethyl)benzoate and (b) [(tetrahydropyran-2-yloxy)methyl]benzoate demonstrating successful protection with THP.

The ^{1}H-NMR spectrum of the product after the saponification reaction of [(tetrahydropyran-2-yloxy)methyl]benzoate is expected to indicate removal of the methyl ester. Indeed, as is depicted in Figure 9, no singlet appears at 3.91 ppm, while all other signals remain unchanged.

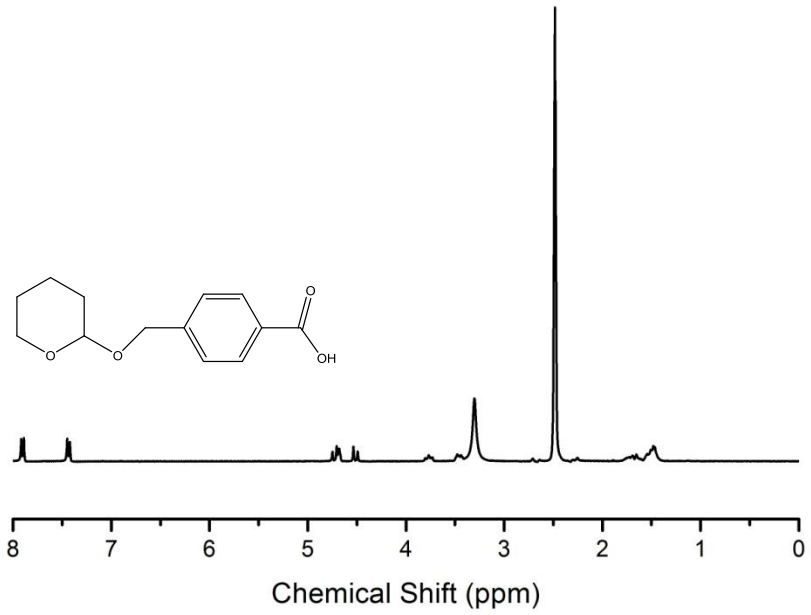

Figure 9. ^{1}H-NMR spectrum of [(tetrahydropyran-2-yloxy)methyl]benzoic acid.

During the benzoyl peroxide synthesis, two [(tetrahydropyran-2-yloxy)methyl]benzoic acid molecules were coupled. As is depicted in Figure 10, as expected, a similar spectrum as for [(tetrahydropyran-2-yloxy)methyl]benzoic acid was obtained. Nevertheless, differences in solubility were observed and therefore the ^{1}H-NMR spectrum of the peroxide was recorded in $CDCl_3$. Furthermore, small quantities of coupling agent were observed, although this was expected not to affect the VDF polymerization. In between 1.5 and 1.0 ppm, traces of N,N'-Dicyclohexylcarbodiimide (DCC) (or the converted N,N'-Dicyclohexylurea (DCU)) were noticed. This was reduced to a minimum by addition of equimolar amounts of [(tetrahydropyran-2-yloxy)methyl]benzoic acid and DCC. The reaction can eventually be prolonged to reduce residual starting material.

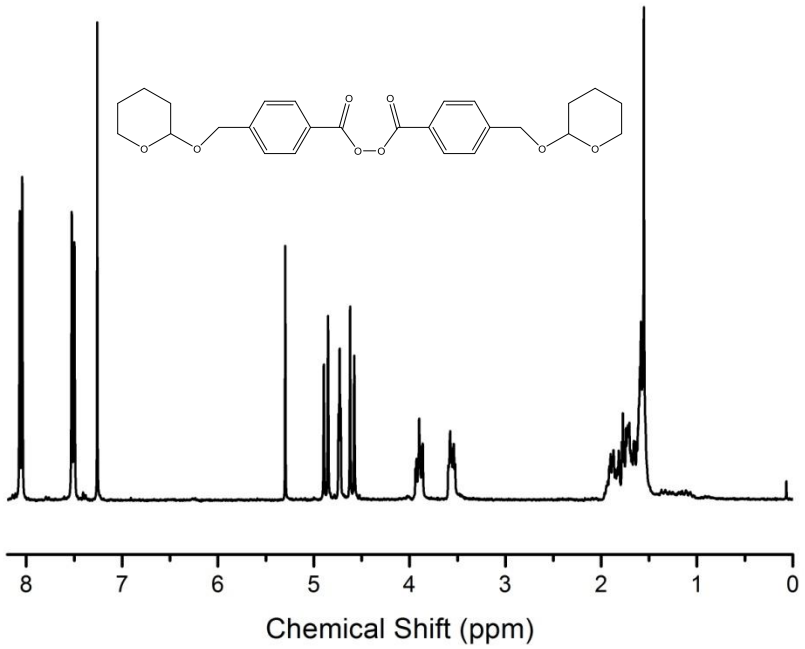

Figure 10. ^{1}H-NMR spectrum of [(tetrahydropyran-2-yloxy)methyl]benzoyl peroxide.

Figure 11 depicts the ^{1}H-NMR spectrum of PVDF after polymerization in the high pressure vessel using [(tetrahydropyran-2-yloxy)methyl]benzoyl peroxide as initiator. Herein, the characteristic signals for PVDF are demonstrated. At 2.87 ppm, the protons of the head-to-tail configuration appeared, whereas the signal at 2.23 ppm demonstrates the tail-to-tail configuration. Chain transfer reactions (*e.g.* intramolecular backbiting, which gives rise to short chain branches) give rise to signals appearing at 6.33 ppm and 1.75 ppm. These signals can be assigned to $-CF_2H$ and $-CF_2CH_3$, respectively.[70] The exclusion of termination by disproportionation is supported by the absence of resonance signals of unsatured bonds. This results in well-defined polymer end-groups (the aromatic protons and the THP protecting group are clearly visible at similar resonances as in the ^{1}H-NMR spectrum of the initiator), since termination can only occur by termination with a primary radical or due to recombination.[71]

According to GPC results, the number average molecular weight was 22.9 kg/mol and a narrow polydispersity was obtained, namely 1.19. The GPC trace of the THP-protected PVDF is depicted in Figure 20 (Appendix).

Acidic cleavage of the THP-protected PVDF was performed using an acetic acid/HCl solution. Absence of the characteristic THP signals in between 2.0 and 1.5 ppm (Figure 11) implies successful removal of the protecting group. Nevertheless, the presence of undefined signals raises questions regarding the purity of the product.

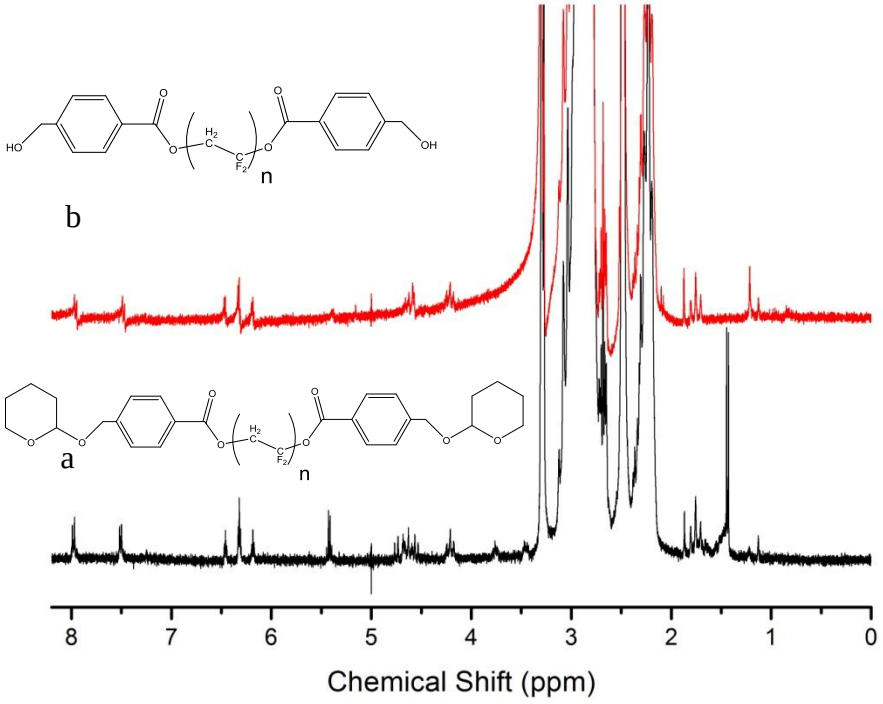

Figure 11. ^{1}H-NMR spectra of (a) THP-protected PVDF and (b) hydroxyl-terminated PVDF.

3.2 Ring opening polymerizations

Stannous(II)octoate was selected as catalyst for the ring opening polymerization of lactide to the PVDF macroinitiator, since it is a widely used catalyst for lactide polymerizations. The reaction was mimicked using benzyl alcohol as initiator in order to optimize the reaction conditions. The solvents used are DMF and cyclohexanone, since PVDF is well-soluble in these solvents (Table 1).

As a control experiment, lactide is polymerized in toluene. In addition, stannous(II)octoate was dissolved in DMF, cyclohexanone, toluene, and DMSO. A white solid was precipitated from these solutions over time, except for the toluene mixture. This is a possible explanation for the full conversion of lactide into PLA in toluene, whereas in all other solvents maximum conversions of 67% were reached (Table 1). The optimum temperature used for lactide polymerization is 110°C, since lower temperatures result in minimum polymerization.

Thus, for the triblock copolymerization, hydroxyl-terminated PVDF was subjected to 110°C, DMF as solvent and reaction times up to 120 hours. These experimental conditions resulted, after precipitation in MeOH/ H_2O (1:1), in polymer, wherefrom the ^{1}H-NMR spectrum is depicted in Figure 12. The characteristic signals for the PVDF chain are preserved, whereas signals for the proton in the PLA backbone appear at 5.18 ppm and for the methyl protons at 1.45 ppm. The signal at 4.18 ppm is assigned to the hydroxyl end-group. The precipitated product was stirred in toluene, and the insoluble particles were filtered. The ^{1}H-NMR spectrum of the residue demonstrates a different ratio of the PVDF signals compared to the PLA signals. Apparently, during the reaction, homopolymers of PLA were formed as well, and these homopolymers were removed by the toluene wash, resulting in the different PVDF/PLA ratio as is depicted in the NMR spectrum.

As a control experiment, lactide polymerizations were performed with stannous(II)octoate and without stannous(II)octoate, furthermore no initiator was added to the reaction mixture. Unfortunately, PLA was formed in the presence of the catalyst, demonstrating that stannous(II)octoate acts as an initiating species as well. Distillation of

stannous(II)octoate was attempted, but without any result due to its high boiling point and viscosity.

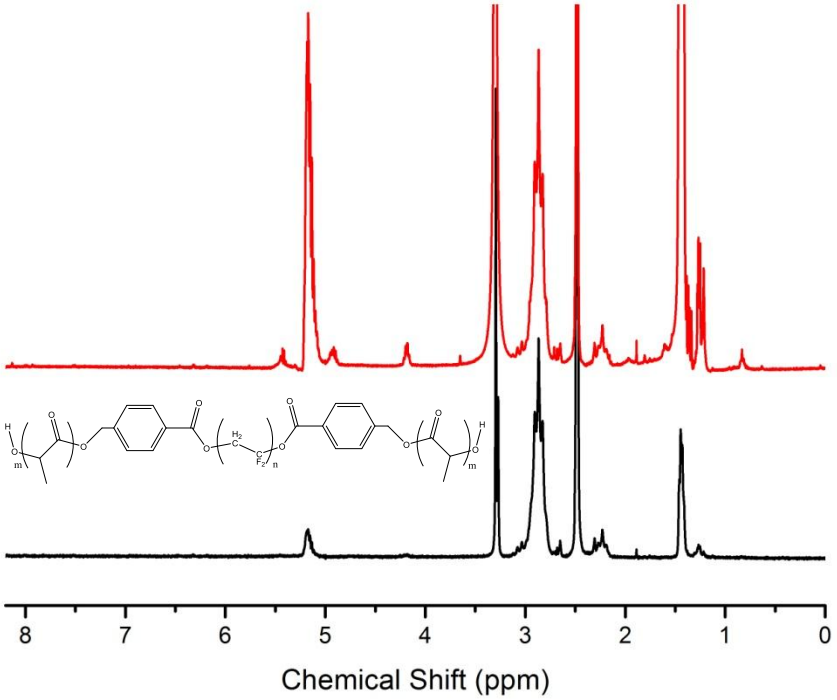

Figure 12. ^{1}H-NMR spectra demonstrating a decrease in ratio PLA to PVDF signals after sequential washing steps, indicating homopolymerization when using stannous(II)octoate as catalyst. The presence of PLA after washing however indicates some lactide coupling to the PVDF macroiniatior.

From here, attention was drawn towards different organocatalysts for the ROP due to their good solubility in DMF, mild reaction conditions, and narrow disperse products. Hydroxyl-terminated PS was used as macroinitiator to mimic the reaction in DMF, where TBD, MTBD, and DBU were used as catalyst. For both MTBD and DBU no polymerization occurred at room temperature in contrast to TBD, where full conversion of lactide was achieved within seconds (Figure 13). This can be attributed to the dual activation mechanism, wherein both hydroxyl end-groups and the monomers are activated in close proximity lowering the energy barrier for the ring opening polymerization. The GPC trace, depicted in Figure 21 (Appendix), also implies that the PS-*b*-PLA was synthesized without any homopolymer formation due the fact that only one peak appeared. However, a control experiment involving only TBD, solvent, and monomer is recommended for excluding initiation by the catalyst. Block

copolymerization with hydroxyl-terminated PVDF was employed with TBD as organocatalyst and a color change (yellow to green/black) during the reaction was observed. This implies a complex formation with TBD in the reaction mixture. A ^{1}H-NMR spectrum of the product demonstrated that a decrease of PLA to PVDF signals was observed after washing the product with toluene. This implies that impurities present in the PVDF macroinitiator product initiate lactide homopolymerization. This is supported by the fact that there are no side-products present after the ROP from the hydroxyl-terminated PS in the presence of TBD.

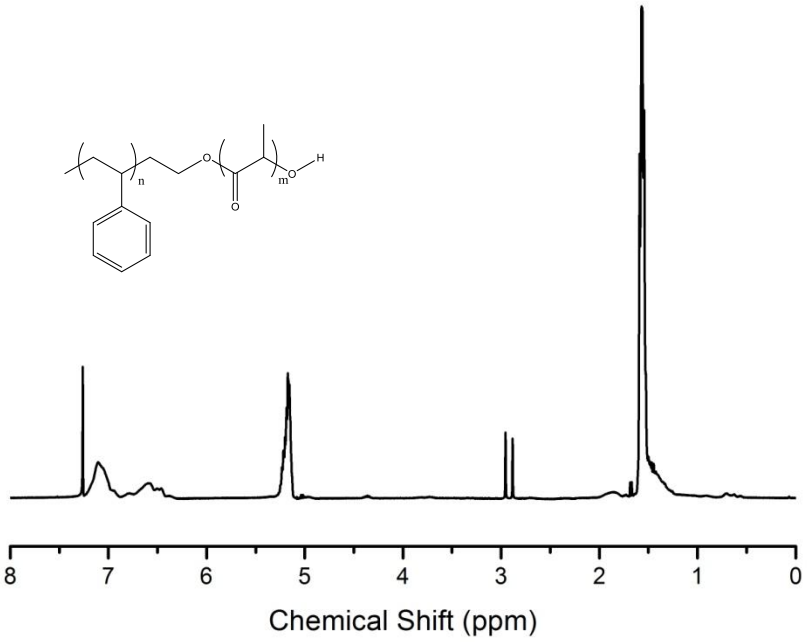

Figure 13. ^{1}H-NMR spectrum of PS-***b***-PLA using TBD as catalyst.

Impurities, which may cause the homopolymerization of PLA, are most probably side-products obtained during the synthesis of the THP-protected benzoyl peroxide. Suggestions to overcome this problem include the use of a smaller protecting group to obtain a recrystallizable initiator (*e.g.* tert-butoxy group instead of THP group) and the use of a different coupling method (*e.g.* avoid the use of DCC as coupling agent and generate a carboxylic chloride to couple *via* Li_2O_2). Post modification of chlorine- and

bromine-terminated PVDF towards hydroxyl-terminated PVDF macroinitiators is also possible, although achieving conversions close to 100% may be challenging.

3.3 Click chemistry

In a first attempt to prepare P3HT-*b*-PVDF-*b*-P3HT block copolymers, hydroxyl-terminated PVDF macroinitiators were end-capped with a thiophene functionality. The precipitation that was observed during the reaction indicated the formation of pyridinium salt, which implies conversion of the hydroxyl end-groups into thiophene end-groups. This is confirmed using ^{1}H-NMR spectroscopy depicted in Figure 14. Herein, the aromatic signals arising at 7.77 ppm, 7.51 ppm, and 7.21 ppm correspond to the thiophene protons and the singlet at 4.84 ppm can be assigned to the two methylene protons. Full conversion of the hydroxyl end-groups cannot be confirmed using this method, however the relative intensities of the aromatic macroinitiator protons and the intensity of methylene signal suggest a decent conversion.

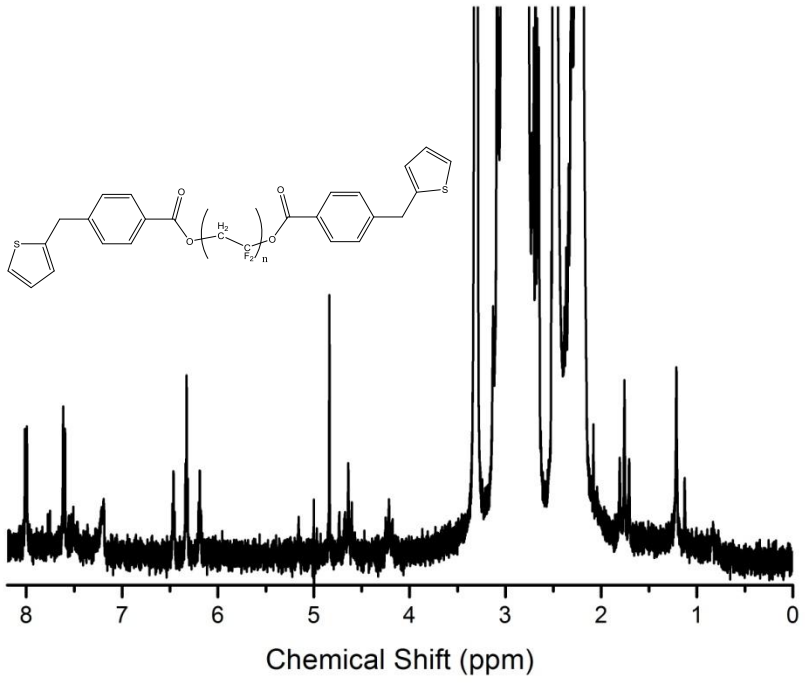

Figure 14. ^{1}H-NMR spectrum of thiophene end-capped PVDF.

From here, triblock copolymerization was attempted *via* oxidative polymerization using iron(III)chloride, as described in the literature.[69] This was not successful and no block copolymerization can be reported. In addition, control experiments using the same reaction conditions and a thiophene carbonyl chloride as initiator demonstrated no homopolymerization.

Development of a new strategy was required and click chemistry was selected as a promising tool to create the novel block copolymers. Independently synthesizing both blocks with narrow polydispersisties and desired functionalities, and subsequently clicking these blocks in high yield was pursued.

Using the procedure described by Voet *et.al.*[1], a new bromine-functionalized initiator for VDF polymerization was developed. Although recrystallization of the 4-(bromomethyl)benzoyl peroxide was employed, small impurities remained as is depicted in Figure 15. Characteristic signals were observed at 8.02 ppm and 7.70 ppm for the aromatic protons and 4.80 ppm for the methylene protons.

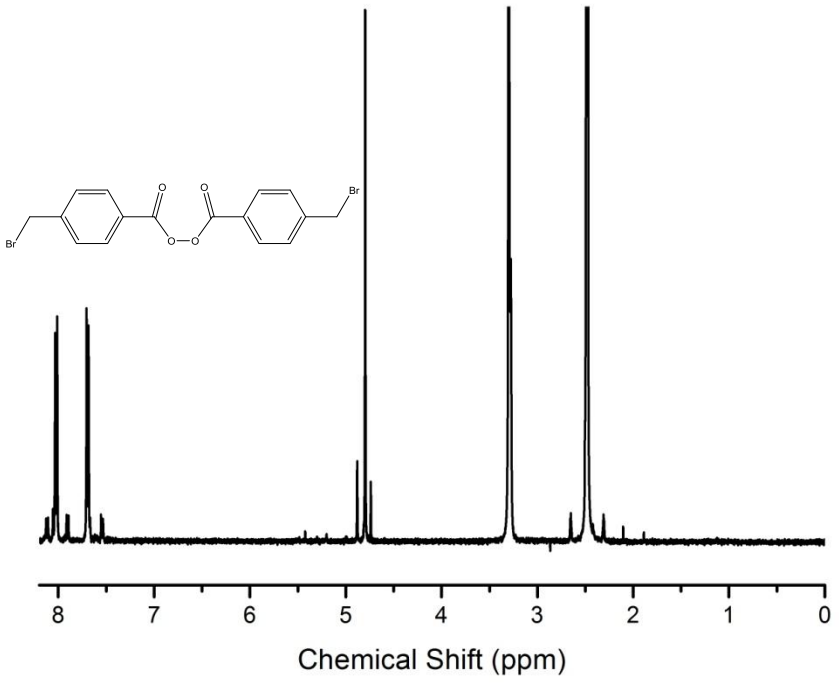

Figure 15. ^{1}H-NMR spectrum of 4-(bromomethyl)benzoyl peroxide. After recrystallization, some starting material was still present, although its influence on the VDF polymerization is expected to be minimal.

The observed impurities were not expected to affect the radical polymerization of VDF. Indeed, ^{1}H-NMR spectroscopy demonstrated PVDF with well-defined bromine end-groups as is depicted in Figure 16. The aromatic proton signals are clearly visible, just as the methylene signal at 4.76 ppm. According to GPC results, the number average molecular weight was calculated to be 23.0 kg/mol and the polydispersity index was 1.14. The GPC trace is depicted in Figure 19 (Appendix).

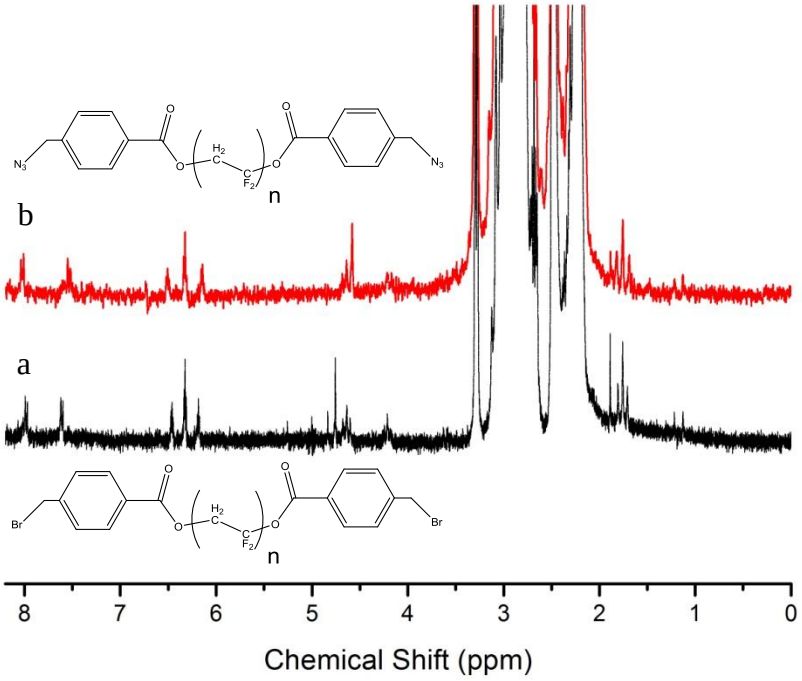

Figure 16. ^{1}H-NMR spectra of (a) bromine-functionalized PVDF and (b) azide-functionalized PVDF.

From here, preparation of the azide-functionalized PVDF was achieved by conversion of the bromine end-groups into azides. An upfield shift of the methylene signal to 4.58 ppm confirmed full conversion as is depicted in the ^{1}H-NMR spectrum of Figure 16. According to GPC results the number average molecular weight was calculated to be 22.4 kg/mol and the polydispersity index was 1.10. These values correspond to the GPC results of the bromine-functionalized precursor. The GPC trace is depicted in Figure 19 (Appendix).

A control experiment with 1-pentyne was employed to investigate the click reaction with the azide-terminated PVDF. ^{1}H-NMR demonstrated a downfield shift of the methylene

signal to 5.66 ppm and disappearance of the -CH_2N_3 signal, indicating successful triazole formation (Figure 17). Unfortunately, due to the high signal-to-noise ratio, the triazole proton is not visible.

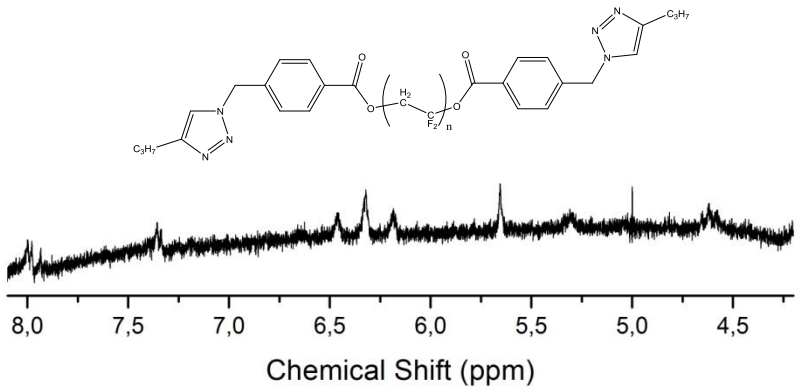

Figure 17. ^{1}H-NMR spectrum of the product of the click reaction of azide-functionalized PVDF with 1-pentyne. Disappearance of -C*H*$_2$N$_3$ signal and appearance of -CH_2-triazole indicates full conversion.

The alkyne-terminated P3HT was synthesized *via* a Grignard metathesis polymerization. Despite extensive washing with various solvents, the final product showed metallic impurities, supposedly nickel arising from the catalyst. Nevertheless, the ^{1}H-NMR spectrum in Figure 18 confirms the formation of ethynyl-terminated P3HT. The relatively high intensity of the signal at 6.98 ppm compared to other signals in that region implies that head-to-tail coupling was predominant, resulting in regioregular P3HT. Furthermore, the proton of the ethynyl end-group was observed at 3.53 ppm, implying successful termination and end-capping of the P3HT backbone with an ethynyl functional group. From the ratio of the integrals of the thiophene ring protons and ethynyl protons, the degree of polymerization was calculated to be 50, corresponding to an average molecular weight of 8000 g/mol.

Most literature reports predicate good solubility of P3HT in THF and toluene. Unfortunately, this was not observed for the P3HT synthesized, probably due to the presence of insoluble impurities. Therefore, soxhlet extractions are recommended to purify the product. Also, additional analysis (*e.g.* MALDI-ToF, GPC, DSC) is required to determine the molecular weight, the molecular weight distribution, and the thermal properties.

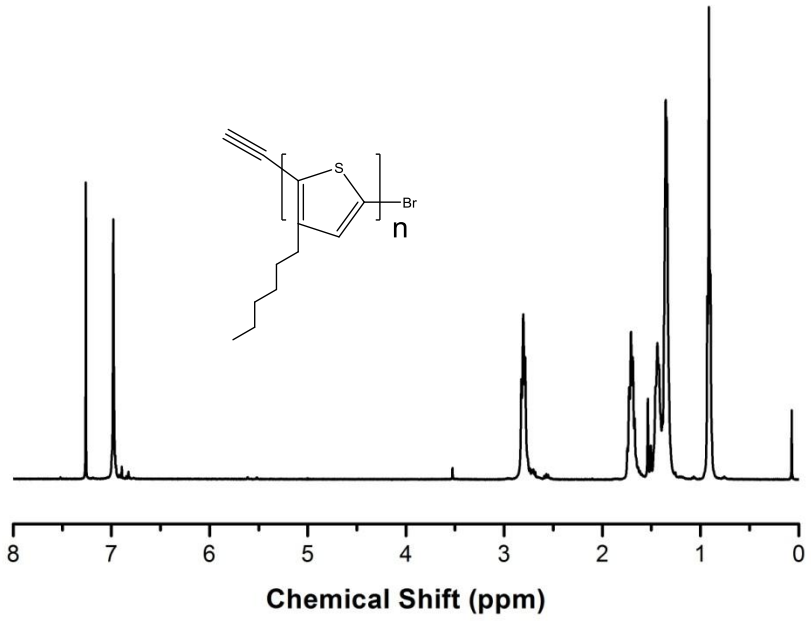

Figure 18. ^{1}H-NMR spectrum of ethynyl-terminated P3HT.

In order to click the PVDF and P3HT chains, triazole formation has to take place. ^{1}H-NMR analysis is expected to demonstrate a signal in between 7.10-7.30 ppm corresponding to the triazole proton together with the characteristic signals of both PVDF and P3HT chains.

Different washing and extraction steps were employed to analyze the product. Rinsing with MeOH, *n*-hexanes, and extraction of the crude product with $CHCl_3$ resulted in a solution containing both PVDF and P3HT. It was expected that subsequent addition of DMF would extract both PVDF and P3HT-*b*-PVDF-*b*-P3HT (if formed), however ^{1}H-NMR spectroscopy demonstrated that only PVDF was extracted. ^{1}H-NMR analysis of the remaining residue after DMF rinse, using $CDCl_3$ as solvent, demonstrated the presence of P3HT only. Thus, the reaction turned out to be unsuccessful.

In future research infrared spectroscopy can be used to investigate the triazole formation, since the characteristic bands of the azide and the alkyne functionalities will disappear accompanied with the appearance of the triazole stretching band.[(72)] Increasing the purity of the starting materials (mainly P3HT) may result in successful coupling, however also

the choice of solvent is crucial. During the described attempt, a mixture of DMF/$CHCl_3$ (1:1) was used. However, the choice of solvent or solvent pairs may be optimized. Furthermore, the P3HT is end-capped with an ethynyl functional group. The reaction mechanism of the CuAAC demonstrates that polarizing the ethynyl bond results in a nucleophilic attack of the azide to the secondary carbon. However, the ethynyl in P3HT is part of a π-conjugated system, which leads to less polarization of the ethynyl bond. Therefore, the secondary carbon is less susceptible for nucleophilic attack on the azide.

4. Conclusions

A hydroxyl-functionalized PVDF was synthesized as described earlier by Kun Li *et. al.*. From this macroinitiator, ring opening polymerization was attempted with the goal to synthesize PLA-*b*-PVDF-*b*-PLA triblock copolymers. Using stannous(II)octoate as catalyst and benzoyl alcohol as initiator, homopolymerizations were observed with a maximum lactide conversion of 67% into PLA. Precipitation of stannous(II)octoate due to poor solubility is probably the main reason for this low conversions, since control experiments demonstrated catalyst precipitation from DMF, cyclohexanone and DMSO. Additionally, lactide polymerizations in toluene with stannous(II)octoate as catalyst resulted in full conversion and no catalyst precipitation was observed. However, due to the poor solubility of PVDF in toluene this solvent system cannot be employed for block copolymerization. No further research attention should be devoted to a system with stannous(II)octoate as catalyst.

Considering organocatalysts, TBD proved to be an efficient catalyst for lactide polymerization in DMF, whereas MTB and DBU demonstrated no activity. Ring opening polymerizations from OH-terminated PS were employed in DMF at room temperature and full conversion was achieved within minutes. The hydroxyl-functionalized PVDF initiated the ring opening polymerization, however the macroinitiator needs to be further purified in order to avoid undesirable homopolymerizations. This can be achieved by multiple reprecipitations or by altering the synthetic route towards the PVDF macroinitiator. In addition, glove box synthesis will provide an inert environment and is therefore recommended, whereas stock solutions are recommended for addition of an accurate amount of catalyst.

Bromine-functionalized and azide-functionalized PVDF macroinitiators were synthesized by tailoring the chemical structure of the initiator and by a post modification of the bromine-functionalized PVDF, respectively. ^{1}H-NMR demonstrated a clear upfield shift for the methylene protons when substituting the bromine for an azide functional group. Additionally, click chemistry by coupling of the azide-functionalized PVDF with 1-pentyne was demonstrated to be successful, according to ^{1}H-NMR, which indicated a

downfield shift of the methylene signal. This implies that click chemistry can be a powerful tool to couple PVDF to alkyne-terminated polymers.

Ethynyl-functionalized P3HT homopolymers were synthesized and characterized by ^{1}H-NMR. A degree of polymerization of approximately 50, corresponding to an average molecular weight of 8000 g/mol, was determined. The high intensity of the signal at 6.98 ppm compared to neighboring signals implies high head-to-tail coupling ratio. The polymers were only soluble in chloroform where literature suggests solubility in THF and toluene as well. Soxhlet extractions are recommended to further purify the product.

A first attempt to synthesize P3HT-*b*-PVDF-*b*-P3HT triblock copolymers failed. Purification of the P3HT precursor is required. Additionally, extending the linking agent between the ethynyl end-group and the polymer backbone should avoid resonance of the ethynyl and will result in more polarization of the ethynyl bond during the reaction.

In future work the crystallization behavior of PLA-*b*-PVDF-*b*-PLA block copolymers will be investigated. The PLA domain is expected to dominate the crystallization process due to the higher crystallization temperature.

Also, the click reaction of P3HT and PVDF will be optimized in future work. This in order to study the electric and magnetic properties of the P3HT-*b*-PVDF-*b*-P3HT block copolymer.

Furthermore, other ethynyl-functionalized polymers will be clicked to PVDF. For example, ethynyl-functionalized PLA homopolymers are easily synthesized and provide an alternative route to the ROP.

5. Literature

(1) Voet, V.; Tichelaar, M.; Tanase-Grecea, S.; Mittelmeijer-Hazeleger, M. M. C.; ten Brinke, G.; Loos, K. *Nanoscale* **2012**.

(2) Davis, G. T.; McKinney, J. E.; Broadhurst, M. G.; Roth, S. C. *Journal of Applied Physics* **1978**, *49*, 4998.

(3) Lovinger, A. J. *Science* **1983**, *220*, 1115.

(4) Freeman, A. J.; Schmid, H. *Magnetoelectric Interaction Phenomena in Crystals*; Gordon and Breach: London, 1995.

(6) Zheng, H.; Wang, J.; Lofland, S. E.; Ma, Z.; Mohaddes-Ardabili, L.; Zhao, T.; Salamanca-Riba, L.; Shinde, S. R.; Ogale, S. B.; Bai, F.; Viehland, D.; Jia, Y.; Schlom, D. G.; Wuttig, M.; Roytburd, A.; Ramesh, R. *Science* **2004**, *303*, 661.

(7) Spaldin, N. A.; Fiebig, M. *Science* **2005**, *309*, 391.

(8) Ramesh, R.; Spaldin, N. A. *Nat. Mater.* **2007**, *6*, 21.

(9) Eerenstein, W.; Mathur, N. D.; Scott, J. F. *Nature* **2006**, *442*, 759.

(10) Kumar, A.; Sharma, G. L.; Katiyar, R. S.; Pirc, R.; Blinc, R.; Scott, J. F. *Journal of Physics-Condensed Matter* **2009**, *21*.

(11) Scott, J. F.; Dearaujo, C. A. P. *Science* **1989**, *246*, 1400.

(12) Wolf, S. A.; Awschalom, D. D.; Buhrman, R. A.; Daughton, J. M.; von Molnar, S.; Roukes, M. L.; Chtchelkanova, A. Y.; Treger, D. M. *Science* **2001**, *294*, 1488.

(13) Bichurin, M. I.; Petrov, V. M.; Kiliba, Y. V.; Srinivasan, G. *Physical Review B* **2002**, *66*.

(14) Nan, C.-W.; Bichurin, M. I.; Dong, S.; Viehland, D.; Srinivasan, G. *Journal of Applied Physics* **2008**, *103*.

(15) Kawai, H. *Japanese Journal of Applied Physics* **1969**, *8*, 975.

(16) Tonelli, A. E.; Schilling, F. C.; Cais, R. E. *Macromolecules* **1982**, *15*, 849.

(17) Bates, F. S.; Fredrickson, G. H. *Physics today* **1999**, *52*, 32.

(18) Blanazs, A.; Armes, S. P.; Ryan, A. J. *Macromolecular Rapid Communications* **2009**, *30*, 267.

(19) Yang, X.; Loos, J. *Macromolecules* **2007**, *40*, 1353.

(20) Hillmyer, M. A. In *Block Copolymers Ii*; Abetz, V., Ed.; Springer-Verlag Berlin: Berlin, 2005; Vol. 190, p 137.

(21) Bates, F. S.; Fredrickson, G. H. *Annual Review of Physical Chemistry* **1990**, *41*, 525.

(22) Matsen, M. W.; Schick, M. *Physical Review Letters* **1994**, *72*, 2660.

(23) Matsen, M. W.; Bates, F. S. *Macromolecules* **1996**, *29*, 1091.

(24) Khandpur, A. K.; Forster, S.; Bates, F. S.; Hamley, I. W.; Ryan, A. J.; Bras, W.; Almdal, K.; Mortensen, K. *Macromolecules* **1995**, *28*, 8796.

(25) Vukovic, I.; Punzhin, S.; Vukovic, Z.; Onck, P.; De Hosson, J. T. M.; ten Brinke, G.; Loos, K. *ACS Nano* **2011**, *5*, 6339.

(26) Cohen, R. E.; Cheng, P. L.; Douzinas, K.; Kofinas, P.; Berney, C. V. *Macromolecules* **1990**, *23*, 324.

(27) Hamley, I. W. In *Developments in Block Copolymer Science and Technology*; Hamley, I. W., Ed.; John Wiley & Sons Ltd: Chichester, 2004.
(28) Pryamitsyn, V.; Ganesan, V. *Journal of Chemical Physics* **2004**, *120*, 5824.
(29) Olsen, B. D.; Segalman, R. A. *Materials Science & Engineering R-Reports* **2008**, *62*, 37.
(30) Ho, V.; Boudouris, B. W.; McCulloch, B. L.; Shuttle, C. G.; Burkhardt, M.; Chabinyc, M. L.; Segalman, R. A. *Journal of the American Chemical Society* **2011**, *133*, 9270.
(31) Matsen, M. W.; Barrett, C. *Journal of Chemical Physics* **1998**, *109*, 4108.
(32) Bhadra, D.; Masud, M. G.; Sarkar, S.; Sannigrahi, J.; De, S. K.; Chaudhuri, B. K. *Journal of Polymer Science Part B-Polymer Physics* **2012**, *50*, 572.
(33) Nan, C. W.; Cai, N.; Shi, Z.; Zhai, J.; Liu, G.; Lin, Y. *Phys. Rev. B* **2005**, *71*.
(34) Vandeleene, S.; Jivanescu, M.; Stesmans, A.; Cuppens, J.; Van Bael, M. J.; Yamada, H.; Sato, N.; Verbiest, T.; Koeckelberghs, G. *Macromolecules* **2010**, *43*, 2910.
(35) Pitet, L. M.; Amendt, M. A.; Hillmyer, M. A. *J. Am. Chem. Soc.* **2010**, *132*, 8230.
(36) Drockenmuller, E.; Li, L. Y. T.; Ryu, D. Y.; Harth, E.; Russell, T. P.; Kim, H. C.; Hawker, C. J. *J. Polym. Sci. Pol. Chem.* **2005**, *43*, 1028.
(37) Guarini, K. W.; Black, C. T.; Zhang, Y.; Kim, H.; Sikorski, E. M.; Babich, I. V. *J. Vac. Sci. Technol. B* **2002**, *20*, 2788.
(38) Maki-Ontto, R.; de Moel, K.; de Odorico, W.; Ruokolainen, J.; Stamm, M.; ten Brinke, G.; Ikkala, O. *Adv. Mater.* **2001**, *13*, 117.
(39) Voet, V. S. D.; Pick, T. E.; Park, S. M.; Moritz, M.; Hammack, A. T.; Urban, J. J.; Ogletree, D. F.; Olynick, D. L.; Helms, B. A. *J. Am. Chem. Soc.* **2011**, *133*, 2812.
(40) Asadi, K.; De Leeuw, D. M.; De Boer, B.; Blom, P. W. M. *Nat. Mater.* **2008**, *7*, 547.
(41) Kam, B.; Li, X. R.; Cristoferi, C.; Smits, E. C. P.; Mityashin, A.; Schols, S.; Genoe, J.; Gelinck, G.; Heremans, P. *Applied Physics Letters* **2012**, *101*.
(42) Laruelle, G.; Nicol, E.; Ameduri, B.; Tassin, J. F.; Ajellal, N. *J. Polym. Sci. Pol. Chem.* **2011**, *49*, 3960.
(43) Asandei, A. D.; Adebolu, O. I.; Simpson, C. P. *Journal of the American Chemical Society* **2012**, *134*, 6080.
(44) Shi, Z. Q.; Holdcroft, S. *Macromolecules* **2004**, *37*, 2084.
(45) Li, K.; Liang, S.; Lu, Y.; Wang, Q. *Macromolecules* **2007**, *40*, 4121.
(46) Destarac, M.; Matyjaszewski, K.; Silverman, E.; Ameduri, B.; Boutevin, B. *Macromolecules* **2000**, *33*, 4613.
(47) Xu, K.; Li, K.; Khanchaitit, P.; Wang, Q. *Chem. Mat.* **2007**, *19*, 5937.
(48) Rostovtsev, V. V.; Green, L. G.; Fokin, V. V.; Sharpless, K. B. *Angewandte Chemie-International Edition* **2002**, *41*, 2596.

(49) Tornoe, C. W.; Christensen, C.; Meldal, M. *Journal of Organic Chemistry* **2002**, *67*, 3057.
(50) Meldal, M. *Macromolecular Rapid Communications* **2008**, *29*, 1016.
(51) Bock, V. D.; Hiemstra, H.; van Maarseveen, J. H. *European Journal of Organic Chemistry* **2006**, 51.
(52) Meldal, M.; Tornoe, C. W. *Chem. Rev.* **2008**, *108*, 2952.
(53) Vukicevic, R.; Schwadtke, U.; Schmucker, S.; Schafer, P.; Kuckling, D.; Beuermann, S. *Polymer Chemistry* **2012**, *3*, 409.
(54) Jeffries-El, M.; Sauvé, G.; McCullough, R. D. *Macromolecules* **2005**, *38*, 10346.
(55) Urien, M.; Erothu, H.; Cloutet, E.; Hiorns, R. C.; Vignau, L.; Cramail, H. *Macromolecules* **2008**, *41*, 7033.
(56) Li, Z. C.; Ono, R. J.; Wu, Z. Q.; Bielawski, C. W. *Chemical Communications* **2011**, *47*, 197.
(57) Lohwasser, R. H.; Thelakkat, M. *Macromolecules* **2012**, *45*, 3070.
(58) Kline, R. J.; McGehee, M. D.; Kadnikova, E. N.; Liu, J.; Fréchet, J. M. J. *Advanced Materials* **2003**, *15*, 1519.
(59) Lan, Y.-K.; Huang, C.-I. *Journal of Physical Chemistry B* **2009**, *113*, 14555.
(60) Garlotta, D. *J. Polym. Environ.* **2001**, *9*, 63.
(61) Vert, M.; Schwarch, G.; Coudane, J. *Journal of Macromolecular Science-Pure and Applied Chemistry* **1995**, *A32*, 787.
(62) Albertsson, A. C.; Varma, I. K. *Biomacromolecules* **2003**, *4*, 1466.
(63) Leenslag, J. W.; Pennings, A. J. *Makromolekulare Chemie-Macromolecular Chemistry and Physics* **1987**, *188*, 1809.
(64) Schwach, G.; Coudane, J.; Engel, R.; Vert, M. *J. Polym. Sci. Pol. Chem.* **1997**, *35*, 3431.
(65) Lohmeijer, B. G. G.; Pratt, R. C.; Leibfarth, F.; Logan, J. W.; Long, D. A.; Dove, A. P.; Nederberg, F.; Choi, J.; Wade, C.; Waymouth, R. M.; Hedrick, J. L. *Macromolecules* **2006**, *39*, 8574.
(66) Hermans, T. M.; Choi, J.; Lohmeijer, B. G. G.; Dubois, G.; Pratt, R. C.; Kim, H.-C.; Waymouth, R. M.; Hedrick, J. L. *Angewandte Chemie-International Edition* **2006**, *45*, 6648.
(67) Sung Ho, K.; Nederberg, F.; Lei, Z.; Wade, C. G.; Waymouth, R. M.; Hedrick, J. L. *Nano Lett.* **2008**, *8*, 294.
(68) Zalusky, A. S.; Olayo-Valles, R.; Wolf, J. H.; Hillmyer, M. A. *Journal of the American Chemical Society* **2002**, *124*, 12761.
(69) de Cuendias, A.; Le Hellaye, M.; Lecommandoux, B.; Cloutet, E.; Cramail, H. *J. Mater. Chem.* **2005**, *15*, 3264.
(70) Pianca, M.; Barchiesi, E.; Esposto, G.; Radice, S. *J. Fluor. Chem.* **1999**, *95*, 71.
(71) Guiot, J.; Ameduri, B.; Boutevin, B. *Macromolecules* **2002**, *35*, 8694.
(72) Pandey, P.; Farha, O. K.; Spokoyny, A. M.; Mirkin, C. A.; Kanatzidis, M. G.; Hupp, J. T.; Nguyen, S. T. *J. Mater. Chem.* **2011**, *21*, 1700.

6. Acknowledgements

I would like to thank Vincent Voet for providing the possibility, the help, and the support, to work on a great project based on an even more amazing polymer.
Prof. dr. Gerrit ten Brinke and Prof. dr. Katja Loos are also greatly acknowledged for their guidance and advise during the project.
I would like to thank Jacob Konieczny and Anton Hofman for their useful tips and for being great lab partners.
And last but not least, I would like to thank the polymer chemistry department of the University of Groningen for creating a pleasant research atmosphere.

7. Appendix

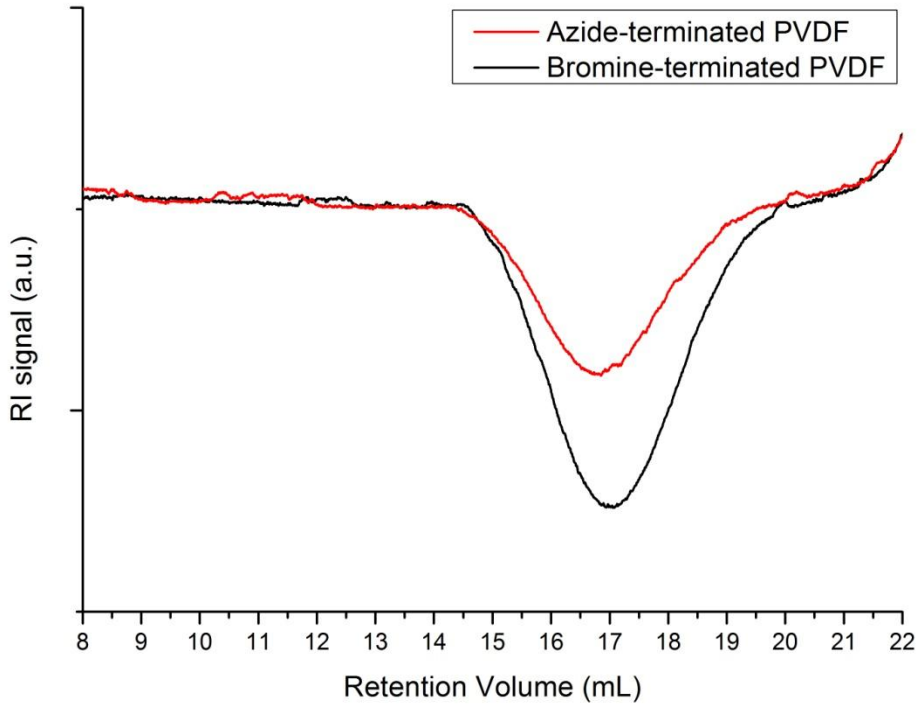

Figure 19. GPC traces of azide-terminated PVDF and bromine-terminated PVDF.

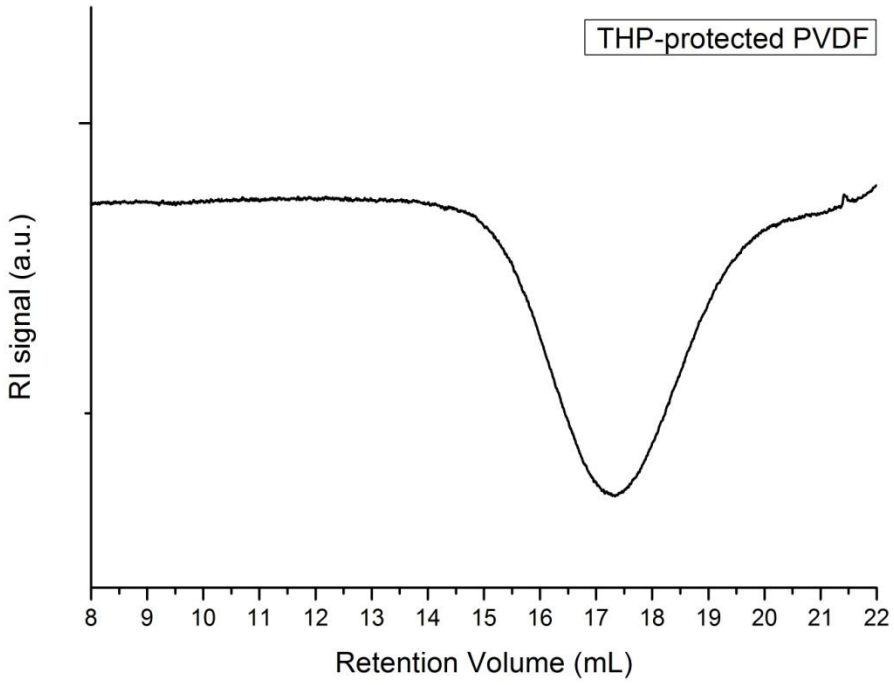

Figure 20. GPC trace of THP-protected PVDF.

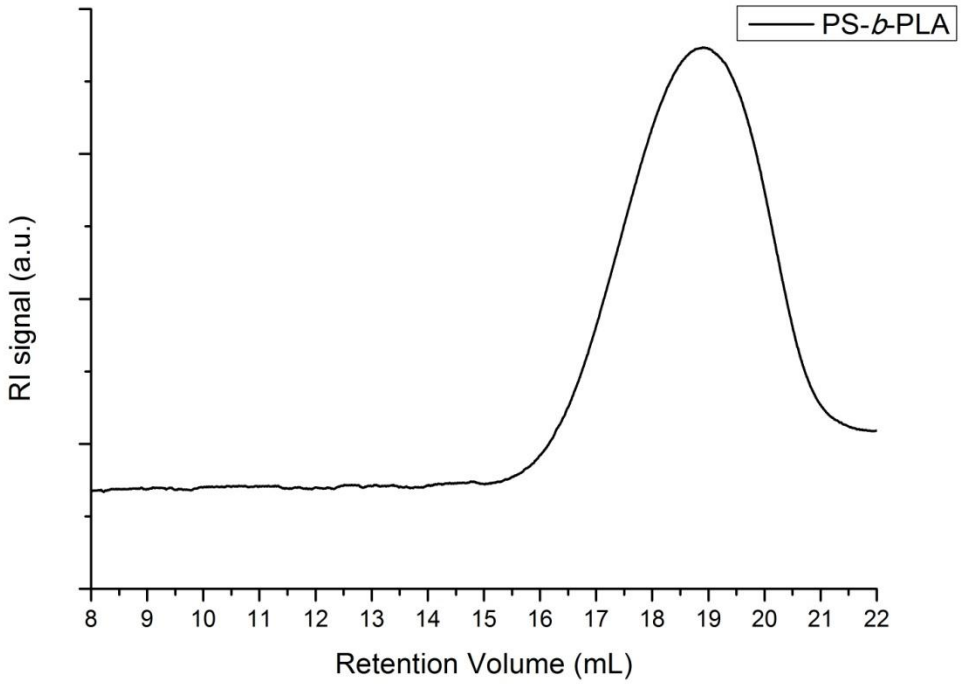

Figure 21. GPC trace of PS-***b***-PLA.